La presenza dell’ordine Camilliano in Piemonte e Liguria: trasformazioni, demolizioni e perdita della memoria di un patrimonio architettonico di età moderna

SINR and Multiuser Efficiency Gap Between MIMO Linear Receivers

G. Alfano, C.-F. Chiasserini, *Fellow, IEEE,* and A. Nordio, *Member, IEEE*

***Abstract*—Due to their low complexity, Minimum Mean Squared Error (MMSE) and Zero-Forcing (ZF) emerge as two appealing MIMO receivers. Although they provide asymptotically the same achievable rate as the signal-to-noise ratio (SNR) grows large, a non-vanishing gap between the signal to interference and noise ratio (SINR) obtained through the two receivers exists, affecting the error and outage probability, and the multiuser efficiency. Interestingly, both the SINR and the multiuser efficiency gaps can be compactly expressed as quadratic forms of random matrices, with a kernel that depends solely on the statistics of the interfering streams. By leveraging [1], we derive the closed-form distribution of such indefinite quadratic forms with random kernel matrix, which turns out to be proportional to the determinant of a matrix containing the system parameters. Then, specializing our result to different fading conditions, we obtain the closed-form statistics of both the SINR gap and the multiuser efficiency gap. Although the focus of this work is on the finite-size statistics, for completeness we also provide some results on the doubly-massive MIMO case. We validate all our derivations through extensive Monte Carlo simulations.**

I. Introduction

Zero Forcing (ZF) and Minimum Mean Squared Error (MMSE) are the most popular linear receivers, due to the desirable trade-off they exhibit between implementation complexity and achievable performance. Interestingly, their supposed performance equivalence in the high Signal-to-Noise Ratio (SNR) regime was partially contradicted in [2]. Therein it was shown that, given a finite number of transmission signal streams with common value of normalized SNR, the output signal-to-interference and noise ratio (SINR) for independent stream decoding, measured in correspondence of an arbitrary branch of the MMSE receiving filter, is equal to the sum of the output SINR of the ZF equalizer on the corresponding branch, plus a *gap* term. The latter is a non-decreasing function of the transmitted SNR [2], [3], and it accounts for the energy that is nulled out by the MMSE but not by the ZF receiver.

According to [2, Eqq. (50, 53)], such a gap between the output SINR values is critical, as it impacts both the outage and the error probability. Moreover, knowledge of the statistics of the gap can serve to upper bound the Interference-to-Noise ratio at the output of an MMSE filter in the high-SINR region [2, Lemma III.2]. Last but not least, an SINR gap between two linear receivers implies the existence of a non-vanishing gap between their Multiuser Efficiency (ME) values. Indeed, the ME is given by the ratio of the achieved SINR to the corresponding SNR in the absence of interference, for each independently decoded stream [4, Eq. (18)]. Deriving closed-form expressions for the statistics of both the SINR and the ME gaps, under different fading conditions, represents one of the main contributions of our work, as also highlighted by the discussion of prior art reported below. Moreover, motivated by the relevance of linear receivers in massive MIMO communications (see e.g., [5], [6] and references therein), we address the SINR and ME gaps statistics in such a setting, for some relevant fading scenarios.

Related work. To date, the probability density function (pdf) of the SINR gap between MMSE and ZF receivers, hereinafter denoted by ν, has been derived in closed form only for asymptotically large transmit power. In [2, Thm. III.1], it was shown that, as the SNR grows large, ν converges with probability one to a random variable with known pdf [7] under the assumption that the intended, as well as the interfering streams, are subject to uncorrelated Rayleigh fading. The remainder of the literature on linear receivers focuses, instead, on the characterization of the output SINR in correspondence of a ZF or a MMSE receiver, but not on the gap between the two of them. The case of a system with a large number of transmit and receive antennas, impaired by transmit-correlated Rayleigh fading, has been investigated in [3]. Irrespectively of the presence of spatial correlation, under Rayleigh fading, the output SINR of the ZF equalizer on a given branch, γ^{zf}, is Gamma distributed [8].

More recent works [9, and references therein] deal with the distribution of γ^{zf} in the line-of-sight (LoS) environment, i.e., when either the desired or the interfering streams [10] experience Rician fading, while the remaining streams experience Rayleigh fading. No results on either γ^{zf} or the SINR gap between the MMSE and the ZF receiver, are available for other channel models. The exact characterization of the output SINR on a given branch of the MMSE receiver, γ^{mmse}, is a more challenging task[1], calling for the separate investigation of γ^{zf} and of the SINR gap, which are easier to handle. ME statistics are, on the other hand, far more complicated than that of the SINR, and, up to date, have been studied only in the large-system case (see [4], [11]).

Aim of the work and contributions. We leverage the fact that both the SINR and the ME gap between the MMSE and the ZF receiver can be expressed in terms of a Hermitian quadratic form, including a vector depending on the desired

G. Alfano is with the Department of Science and Applied Technology, Politecnico di Torino, 10129 Italy e-mail: d020860@polito.it

C.-F. Chiasserini is with Department of Electronics, Politecnico di Torino, 10129 Italy, and a Research Associate at CNR-IEIIT, e-mail: chiasserini@polito.it

A. Nordio is with Wireless Communications Systems Group, CNR-IEIIT, Torino, 10129 Italy, e-mail: alessandro.nordio@ieiit.cnr.it

[1]The pdf of γ^{mmse} is available when both desired and interfering signals are Rayleigh faded [12], [13]. A closed-form expression for its moments can be found for the case of Rice-faded useful stream/Rayleigh-faded interference in [14]. Large-deviations behavior of γ^{mmse} is investigated in [15].

signal stream and a kernel matrix depending on the interfering streams only. In particular, the SINR gap can be cast, in all fading cases of practical interest, as a positive-definite quadratic form that can be analyzed using theoretical tools of multivariate analysis. The expression of the ME gap, instead, corresponds to that of an indefinite quadratic form, and will be studied exploiting some recently derived tools [1]. Our analysis provides a *handy, yet elegant, closed-form expression* for both the SINR and the ME gap, given by the product of a constant by a matrix determinant. In the rest of the work, Sec. III introduces the system model and defines the SINR and the ME gap. They are successively expressed in terms of quadratic forms in random kernel matrices, and useful results from the literature are recalled.

Then we focus on the case of a Rayleigh-faded intended stream[2]. Under this assumption, in Sec. IV we first provide a non-asymptotic result complementing the fundamental one of [2, Thm. III.1], by giving the gap distribution for Rayleigh-faded interfering streams but *arbitrary* rather than *arbitrarily large* SINR values. The case of transmit-correlated Rayleigh fading, possibly corresponding to spatially-clustered interferers, is addressed in the same vein. Next, we derive the corresponding statistics in the case of Rician-faded interfering streams, for arbitrary rank and eigenvalues multiplicity of LoS matrix. Such a scenario is representative of a worst-case cellular transmission, where the useful stream comes, e.g., from the cell edge and dominant interferers have LoS path toward the base station. Finally, we evaluate the pdf of the SINR gap for the case where interfering streams undergo multiple Rayleigh scattering[3]. This last scenario is of particular interest in small-cells networks. Indeed, it adequately represents, with no approximation in the channel statistics, the case where interfering signals come from non co-located single-antenna equipped transmitters, whose signals may undergo multiple scattering phenomena. Comparative performance analysis of MMSE and ZF receivers, based on the newly derived results, and contrasted with numerical simulation, complete the work. In particular, as an example of application of our results, we evaluate the key statistics of the SINR gap, relating the value of the symbol error probability and that of the outage probability of an MMSE receiver with the corresponding performance indices in the case of ZF (Secs. V and VI).

As for the ME gap, Sec. VII presents the pdf of the ME gap in closed form and the mathematical tools needed for its derivation. Sec. IX tackles the case of doubly-massive MIMO communications and provides results and discussions on the SINR and ME gaps. These analytical results are validated through extensive simulations (Secs. VIII and IX).

II. Notation

Boldface uppercase and lowercase letters denote matrices ad vectors, respectively. $\mathbf{I}$ is the identity matrix. The determinant

[2]A Rayleigh-faded useful stream allows for closed-form expressions of the relevant statistics. Other fading distributions allow for saddle-point approximations, which are accurate only as the system size grows large [1].

[3]See [16] for the statistical analysis of a multiple scattering system, and [17], [18] for practical justification and information-theoretic performance of such channels, as the number of scattering stages vary. Also, a preliminary analysis of the Rayleigh quotient can be found in [19].

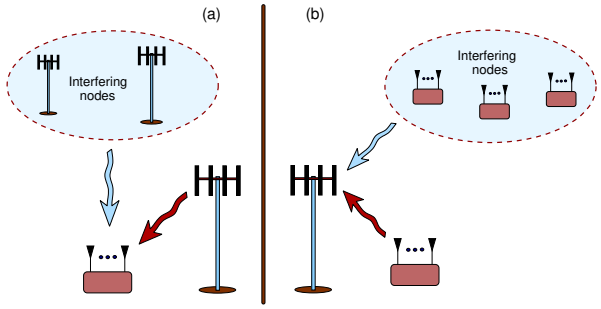

Fig. 1. (a) Downlink scenario where a user or a relay node receive a useful signal from a base station as well as interference from other nodes; (b) Uplink scenario where a relay or user node transmit a useful stream to a base station and interference may be generated by other nearby nodes.

and the conjugate transpose of the generic matrix $\mathbf{A}$ are denoted by $|\mathbf{A}|$ and $\mathbf{A}^{\mathsf{H}}$, respectively, while $[\mathbf{A}]_{i,j}$ is the (i,j)-th element of $\mathbf{A}$. For any $m \times m$ Hermitian matrix $\mathbf{A}$ with distinct eigenvalues $a_1, \ldots, a_m$, the Vandermonde determinant is defined as: $\mathcal{V}(\mathbf{A}) = \prod_{1 \le k < \ell \le m} (a_\ell - a_k)$. The Vandermonde determinant is sometimes denoted by $\mathcal{V}(\mathbf{a})$, in order to stress the dependence on the vector of eigenvalues $\mathbf{a} = [a_1, \ldots, a_m]^{\mathsf{T}}$. $G_{a,b}^{c,d}(\cdot|\cdot)$, with integer parameters a, b, c, d, denotes the Meijer-G function [20, Ch. 8]. $\mathbb{E}_a[\cdot]$ represents the average operator with respect to the random variable a. The generalized hypergeometric function is denoted by ${}_pF_q(\mathbf{a}; \mathbf{b}; x)$, and the complex multivariate Gamma function is defined as [21]: $\Gamma_p(q) = \pi_p \prod_{\ell=1}^{p} (q-\ell)!$, with p and q non-negative integers such that $p \le q$, and $\pi_p = \pi^{p(p-1)/2}$. Finally, $f_a(a)$, $f_{\mathbf{a}}(\mathbf{a})$, and $f_{\mathbf{A}}(\mathbf{A})$ denote the pdf of a scalar, multivariate, and matrix-variate random variable, respectively, while $F_a(a)$ denotes the cumulative distribution function (cdf) of the random variable a.

III. System Model and Mathematical Preliminaries

We focus on a wireless network composed of a receiver equipped with multiple antennas, a transmitter equipped with one or more antennas, and, possibly, a set of interferers. Such model reflects practical scenario as depicted in Fig. 1 where (a) and (b) refer to, respectively, downlink and uplink communications in a cellular network. Denoting by n_{r} the number of antennas at the receiver and by n_{t} the overall number of transmitting antennas (i.e., irradiating either useful or interfering signals), the received signal can be written as

$$\mathbf{y} = \sqrt{\delta}\mathbf{h}x + \widehat{\mathbf{H}}\widehat{\mathbf{\Delta}}\hat{\mathbf{x}} + \mathbf{n}$$

where

- $\mathbf{y}$ is the received signal vector of length n_{r};
- x is the intended transmitted symbol with zero mean and unitary variance, $\mathbf{h}$ is the channel vector, and δ is the SNR on the transmitter-receiver link;
- $\hat{\mathbf{x}}$ is the vector of zero mean interfering symbols with covariance $\mathbb{E}[\hat{\mathbf{x}}\hat{\mathbf{x}}^{\mathsf{H}}] = \mathbf{I}$, $\widehat{\mathbf{H}}$ is the channel matrix on the interferers-receiver links, and $\widehat{\mathbf{\Delta}} = \mathrm{diag}(\sqrt{\hat{\delta}_1}, \ldots, \sqrt{\hat{\delta}_{n_{\mathrm{t}}-1}})$ is the diagonal matrix of the amplitudes of the interfering signals;

- $\mathbf{n}$ is a Gaussian random vector representing additive noise with covariance $\mathbb{E}[\mathbf{n}\mathbf{n}^{\mathsf{H}}] = \mathbf{I}$.

We also define $\mathbf{H} = [\mathbf{h}, \widehat{\mathbf{H}}]$ as the $n_{\mathrm{r}} \times n_{\mathrm{t}}$ random channel matrix, which we assume to be available at the receiver, and we define $\mathbf{\Delta} = \mathrm{diag}(\sqrt{\delta}, \sqrt{\hat{\delta}_1}, \ldots, \sqrt{\hat{\delta}_{n_{\mathrm{t}}-1}})$ as the amplitude of the useful and interfering signals. Note that this is a fair assumption since in advanced systems, such as 5G, the base station can accurately estimate the channel state information related to each user thanks to the Sounding Reference Signal (SRS) transmitted by every UE in uplink. If a data transfer is in place, also the Demodulation Reference Signal (DMRS) can be used to support MIMO transmissions. In downlink, the user can exploit the Channel State Information Reference Signal (CSI-RS) transmitted by base stations and obtain a channel estimation, which is quite accurate in the case of stationary or slowly moving users.

In case of independent stream decoding, the output SINR corresponding to the useful signal can be expressed for the MMSE and, respectively, for the ZF receiver as [22, Ch. 6]:

$$\gamma^{\mathrm{mmse}} = \frac{1}{(\mathbf{I}+\mathbf{\Delta}\mathbf{H}^{\mathsf{H}}\mathbf{H}\mathbf{\Delta})^{-1}_{1,1}} - 1,\ \gamma^{\mathrm{zf}} = \frac{1}{(\mathbf{\Delta}\mathbf{H}^{\mathsf{H}}\mathbf{H}\mathbf{\Delta})^{-1}_{1,1}}\,. \quad (1)$$

The difference of the above quantities is referred to as *SINR gap* and is defined as [2], [3]

$$\nu = \gamma^{\mathrm{mmse}} - \gamma^{\mathrm{zf}}\,. \quad (2)$$

As mentioned, the SINR gap is a non-decreasing function of the SNR, accounting for the energy nulled out by the ZF but not by the MMSE receiver, and it can be modeled as a random variable supported on the non-negative real axis [2].

In turn, the ME achieved by the useful stream is given by the ratio between the corresponding SINR and the SNR in absence of other-stream interference, i.e., [4, Eq. (18)]

$$\eta^{\mathrm{mmse}} = \frac{\gamma^{\mathrm{mmse}}}{\delta\|\mathbf{h}\|^2}\,, \quad \eta^{\mathrm{zf}} = \frac{\gamma^{\mathrm{zf}}}{\delta\|\mathbf{h}\|^2}\,. \quad (3)$$

In analogy with the SINR gap, the *multiuser efficiency gap* can be defined from (2)-(3), as

$$\mu = \eta^{\mathrm{mmse}} - \eta^{\mathrm{zf}} = \frac{\nu}{\delta\|\mathbf{h}\|^2}\,. \quad (4)$$

The statistics of both ν and μ can be related to those of properly cast Hermitian quadratic forms in random matrices. Let $\mathbf{G} = \widehat{\mathbf{H}}\widehat{\mathbf{\Delta}}$; then the SINR gap defined in (2), is given by the quadratic form [2, Eq. (26)]

$$\nu = \delta\mathbf{h}^{\mathsf{H}}\mathbf{U}\left(\mathbf{I}_{n_{\mathrm{t}}-1} + \mathbf{\Lambda}\right)^{-1}\mathbf{U}^{\mathsf{H}}\mathbf{h}\,, \quad (5)$$

where $\mathbf{G} = \mathbf{U}\mathbf{\Lambda}^{1/2}\mathbf{V}^{\mathsf{H}}$ is a decomposition of $\mathbf{G}$, with $\mathbf{U}$ being a complex matrix of size $n_{\mathrm{r}} \times (n_{\mathrm{t}}-1)$ with orthogonal columns (i.e., $\mathbf{U}^{\mathsf{H}}\mathbf{U} = \mathbf{I}_{n_{\mathrm{t}}-1}$); $\mathbf{\Lambda} = \mathrm{diag}(\lambda_1, \ldots, \lambda_{n_{\mathrm{t}}-1})$ is a square diagonal matrix of size $n_{\mathrm{t}} - 1$ with its diagonal including the non-zero eigenvalues of $\mathbf{G}^{\mathsf{H}}\mathbf{G}$, and $\mathbf{V}$ is a square unitary matrix of size $n_{\mathrm{t}} - 1$. Details on how to derive (5) from (1) are reported in Appendix A.

The law of a quadratic form $\mathbf{h}^{\mathsf{H}}\mathbf{A}\mathbf{h}$ as in (5) has been studied in the literature, when the elements of $\mathbf{h}$ are i.i.d. and zero-mean, Gaussian distributed. A characterization of such quadratic form for MIMO systems is provided e.g., in [23] where the kernel matrix $\mathbf{A}$ is considered deterministic. We extend this result to the case of a random kernel matrix since, in our scenario, $\mathbf{A}$ depends on the random matrix $\mathbf{G}$.

The ME gap becomes the ratio of two quadratic forms,

$$\mu = \frac{\mathbf{h}^{\mathsf{H}}\mathbf{A}\mathbf{h}}{\|\mathbf{h}\|^2}\,, \quad (6)$$

where, according to (4) and (5), $\mathbf{A} = \mathbf{U}\left(\mathbf{I}_{n_{\mathrm{t}}-1} + \mathbf{\Lambda}\right)^{-1}\mathbf{U}^{\mathsf{H}}$, has eigenvalues

$$\mathbf{a} = \Big[\underbrace{\alpha_1, \ldots, \alpha_{n_{\mathrm{t}}-1}}_{\boldsymbol{\alpha}}, \underbrace{0, \ldots, 0}_{n_{\mathrm{r}}-n_{\mathrm{t}}+1}\Big] \quad (7)$$

with $\alpha_i = (1+\lambda_i)^{-1}$, $i = 1, \ldots, n_{\mathrm{t}} - 1$. Being both the numerator and the denominator in (6) quadratic forms in $\mathbf{h}$, μ can be expressed as a Rayleigh quotient [24], whose statistics boil down to that of a properly cast indefinite quadratic form.

Our setting (6) requires an investigation of μ when $\mathbf{A}$ and $\mathbf{h}$ are randomly distributed. To this end, we consider the cdf of the ME gap conditioned to matrix $\mathbf{A}$, i.e., $F_{\mu|\mathbf{A}}(z) = \mathbb{P}(\mu \le z|\mathbf{A})$. When $\mathbf{A}$ is a deterministic matrix, different expressions for the pdf of μ are provided in [1], depending on the multiplicity of the eigenvalues of $\mathbf{A}$; in the remainder of the paper, we address instead the case of random $\mathbf{A}$. Most of the results will be derived by using the following Lemmas, which have general validity beyond the scope of this paper.

Lemma 3.1: Let $\mathcal{L}_y\{\cdot\}$ be a linear operator acting on functions of the variable y. Let $\mathbf{\Xi}$ be an $n \times n$ matrix defined as

$$[\mathbf{\Xi}]_{i,j} = \begin{cases} c_{i,j} & 1 \le i \le n, i \ne k, 1 \le j \le n \\ \xi_j(y) & i = k, 1 \le j \le n \end{cases}$$

where $c_{i,j}$ are constant w.r.t. y, and $\xi_j(y)$ are arbitrary functions. Then $\mathcal{L}_y\{|\mathbf{\Xi}|\} = |\widetilde{\mathbf{\Xi}}|$ where

$$[\widetilde{\mathbf{\Xi}}]_{i,j} = \begin{cases} c_{i,j} & 1 \le i \le n, i \ne k, 1 \le j \le n \\ \mathcal{L}_y\{\xi_j(y)\} & i = k, 1 \le j \le n\,. \end{cases}$$

Proof: The determinant of $\mathbf{\Xi}$ can be evaluated by using the Laplace expansion over the k-th column of $\mathbf{\Xi}$. We have $|\mathbf{\Xi}| = \sum_{i=1}^{n} C_j \xi_j(y)$ where C_j is the (constant w.r.t. y) (k,j)-th cofactor of $\mathbf{\Xi}$. Since $\mathcal{L}_y\{\cdot\}$ is linear we have $\mathcal{L}_y\{|\mathbf{\Xi}|\} = \sum_{i=1}^{n} C_j \mathcal{L}_y\{\xi_j(y)\}$ which coincides with the Laplace expansion of $|\widetilde{\mathbf{\Xi}}|$ over the k-th column of $\widetilde{\mathbf{\Xi}}$. ∎

Lemma 3.2: [25, Corollary I] Let $\mathbf{\Phi}$ and $\mathbf{\Psi}$ be two $n \times n$ arbitrary matrices such that $[\mathbf{\Psi}]_{i,j} = \psi_i(x_j)$ and $[\mathbf{\Phi}]_{i,j} = \phi_i(x_j)$. Also, let $\zeta(\cdot)$ be an arbitrary function. Then the integral $\int_{\mathcal{X}} |\mathbf{\Phi}||\mathbf{\Psi}| \prod_{i=1}^{n} \zeta(x_i)\,\mathrm{d}\mathbf{x} = |\mathbf{\Theta}|$ where $\mathcal{X} = \{b \ge x_1 \ge x_2 \ge \cdots \ge x_n \ge a\}$ is the integration domain and $[\mathbf{\Theta}]_{i,j} = \int_a^b \psi_i(x)\phi_j(x)\zeta(x)\,\mathrm{d}x$.

The notations we use are summarized in Table I.

IV. Statistical Characterization of the SINR gap

We now statistically characterize the SINR gap, ν, under different assumptions on the statistics of the diagonal matrix $\mathbf{\Lambda}$ in (5), and assuming that $\mathbf{h} \sim \mathcal{CN}(0, \mathbf{I}_{n_{\mathrm{r}}})$, i.e., the received signal streams are affected by uncorrelated Rayleigh fading. We will maintain the latter assumption on the intended signal stream throughout the work, while different distributions of the fading affecting the interfering streams will be considered.

TABLE I
DESCRIPTION OF THE MAIN NOTATIONS USED IN THE WORK

Notation	Description
n_t, n_r	No. transmit and receiver antennas
$n_\mathrm{t}-1$	No. of interfering antennas
τ_i	Shorthand notation for $n_\mathrm{r}-n_\mathrm{t}+i$, $i\in\mathbb{N}$
δ	Useful signal power
$\mathbf{h}$	Channel vector of the useful signal
$\widehat{\mathbf{H}}$	Channel matrix of the interfering signals
$\widehat{\mathbf{\Delta}}$	Amplitudes of the interfering signals
$\mathbf{\Lambda}$	Eigenvalues of $\mathbf{G}^\mathsf{H}\mathbf{G}$, ($\mathbf{G}=\widehat{\mathbf{H}}\widehat{\mathbf{\Delta}}$)
$\mathbf{L}$	Eigenvalues of $\widehat{\mathbf{H}}^\mathsf{H}\widehat{\mathbf{H}}$
ν, μ	SINR and ME gap
$f_\nu(y), F_\nu(y)$	pdf and cdf of the SINR gap
$f_\mu(y), F_\mu(y)$	pdf and cdf of the ME efficiency gap

Below, we first provide the expression of the conditional distribution $f_{\nu|\mathbf{\Lambda}}(y)$. Then, under some hypothesis on the structure of $f_{\mathbf{\Lambda}}(\mathbf{\Lambda})$, we obtain $f_\nu(y)$. We start by proving the following lemma on the SINR gap distribution $f_{\nu|\mathbf{\Lambda}}(y)$, which holds under the assumption of Rayleigh fading afflicting the main signal stream and given the interfering streams fading law. The lemma provides the pdf of the SINR gap in a simple, yet elegant, form, as the product of a constant by the determinant of the matrix representing the system.

Lemma 4.1: Consider independent stream decoding and the SINR gap ν as defined in (5). Then ν is a random variable whose conditional law, with respect to the fading distribution affecting the interfering streams (i.e., conditioned to $\mathbf{\Lambda}$), is:

$$f_{\nu|\mathbf{\Lambda}}(y)=\frac{s|\mathbf{T}|}{\mathcal{V}(\mathbf{\Lambda})}\,, \tag{8}$$

where $s=(-1)^{(n_\mathrm{t}-1)(n_\mathrm{t}-2)/2}$ and $\mathbf{T}$ is a $(n_\mathrm{t}-1)\times(n_\mathrm{t}-1)$ matrix, with generic element

$$[\mathbf{T}]_{i,j}=t_i(\lambda_j)=\begin{cases}(1+\lambda_j)^{n_\mathrm{t}-i-1} & \begin{array}{l}1\le j\le n_\mathrm{t}-1\\ 1\le i\le n_\mathrm{t}-2\end{array}\\ \frac{1+\lambda_j}{\delta}\mathrm{e}^{-y(1+\lambda_j)/\delta} & \begin{array}{l}1\le j\le n_\mathrm{t}-1\\ i=n_\mathrm{t}-1\end{array}\end{cases} \tag{9}$$

Proof: In [26] it is shown that if $\mathbf{V}$ is an $m\times n$ ($m<n$) complex Gaussian random matrix with zero mean, constant covariance matrices $\mathbf{\Sigma}_1$ and $\mathbf{\Sigma}_2$, and density

$$f_{\mathbf{V}}(\mathbf{V})=\frac{\exp\left(-\mathsf{Tr}\{\mathbf{\Sigma}_1^{-1}\mathbf{V}\mathbf{\Sigma}_2^{-1}\mathbf{V}^\mathsf{H}\}\right)}{\pi^{nm}|\mathbf{\Sigma}_1|^n|\mathbf{\Sigma}_2|^m}\,.$$

Then the density of the quadratic form $\mathbf{Y}=\mathbf{V}\mathbf{V}^\mathsf{H}$ is

$$f_{\mathbf{Y}|\mathbf{\Sigma}_1,\mathbf{\Sigma}_2}(\mathbf{Y})=\frac{\pi^{m(m-1)/2}|\mathbf{S}|}{|\mathbf{\Sigma}_1|^m\mathcal{V}(\mathbf{Y})\mathcal{V}(\mathbf{\Sigma}_2)}\,. \tag{10}$$

The elements of $\mathbf{S}$ in (10) can be written as:

$$[\mathbf{S}]_{i,j}=\begin{cases}p_j^{i-1} & 1\le j\le n,\ 1\le i\le n-m\\ p_j^{n-m-1}\mathrm{e}^{-\frac{y_{i-n+m}}{p_j}} & 1\le j\le n,\ n-m+1\le i\le n\end{cases}$$

with $[p_1,\ldots,p_n]$ being the eigenvalues of $\mathbf{\Sigma}_2$ and $[y_1,\ldots,y_m]$ the eigenvalues of $\mathbf{Y}$. Next, let $\mathbf{\Sigma}_2=\delta\left(\mathbf{I}_{n_\mathrm{t}-1}+\mathbf{\Lambda}\right)^{-1}$ and $\mathbf{v}=\mathbf{h}^\mathsf{H}\mathbf{U}\mathbf{\Sigma}_2^{1/2}$. Since $\mathbf{h}\sim\mathcal{CN}(0,\mathbf{I}_{n_\mathrm{r}})$, by the invariance of the complex Gaussian distribution to linear transformations and by the fact that $\mathbf{U}^\mathsf{H}\mathbf{U}=\mathbf{I}_{n_\mathrm{t}-1}$, then $\mathbf{v}\sim\mathcal{CN}(0,\mathbf{\Sigma}_2)$. It immediately follows that, when $\mathbf{V}$ is replaced by the $1\times(n_\mathrm{t}-1)$ vector $\mathbf{v}^\mathsf{H}$ (i.e., $m=1$, $n=n_\mathrm{t}-1$, $\mathbf{\Sigma}_1=1$), the term $\mathbf{Y}$ reduces to a scalar, thus $\mathcal{V}(\mathbf{Y})=1$, and the density in (10) corresponds to that of the quadratic form $\nu=\|\mathbf{v}\|^2$. Hence, it can be written as:

$$f_{\nu|\mathbf{\Sigma}_2}(y)=\frac{|\mathbf{S}|}{\mathcal{V}(\mathbf{\Sigma}_2)}\,. \tag{11}$$

Since *(i)* the eigenvalues of $\mathbf{\Sigma}_2$ are $p_j=\delta\,(1+\lambda_j)^{-1}$, $j=1,\ldots,n_\mathrm{t}-1$, and *(ii)* the variable $\mathbf{\Sigma}_2$ depends on the random matrix $\mathbf{\Lambda}$ only (hence, $f_{\nu|\mathbf{\Sigma}_2}(y)=f_{\nu|\mathbf{\Lambda}}(y)$), we can write

$$\mathcal{V}(\mathbf{\Sigma}_2)=\prod_{1\le i<j<n_\mathrm{t}-1}p_j-p_i=\frac{(-\delta)^{(n_\mathrm{t}-1)(n_\mathrm{t}-2)/2}\mathcal{V}(\mathbf{\Lambda})}{|\mathbf{I}+\mathbf{\Lambda}|^{n_\mathrm{t}-2}}\,.$$

By exploiting the result in (11) and observing that the product of two determinants of equal size matrices is the determinant of the matrix product, after some algebra we obtain (8). ■

Equipped with (8), we derive $f_\nu(y)$ for the general case, encompassing a number of fading scenarios, for which detailed expressions will be listed in the following.

Proposition 4.1: Let $\mathbf{G}$ be a random channel matrix of interfering streams of size $n_\mathrm{r}\times(n_\mathrm{t}-1)$, $n_\mathrm{r}\ge n_\mathrm{t}$. Let $\mathbf{\Lambda}=\mathrm{diag}(\lambda_1,\ldots,\lambda_{n_\mathrm{t}-1})$ be the matrix of the unordered eigenvalues of $\mathbf{G}^\mathsf{H}\mathbf{G}$. Assume that the distribution of $\mathbf{\Lambda}$ is given by

$$f_{\mathbf{\Lambda}}(\mathbf{\Lambda})=\frac{\mathcal{K}}{(n_\mathrm{t}-1)!}\mathcal{V}(\mathbf{\Lambda})|\mathbf{\Phi}|\prod_{i=1}^{n_\mathrm{t}-1}\psi(\lambda_i)\,, \tag{12}$$

where $\mathcal{K}$ is the normalizing factor of the pdf, $\mathbf{\Phi}$ is an arbitrary $(n_\mathrm{t}-1)\times(n_\mathrm{t}-1)$ matrix with $[\mathbf{\Phi}]_{i,j}=\phi_i(\lambda_j)$, $i,j=1,\ldots,n_\mathrm{t}-1$, and $\psi(\cdot)$ is an arbitrary function. Then, recalling that $s=(-1)^{(n_\mathrm{t}-1)(n_\mathrm{t}-2)/2}$ is a constant as defined after (8), the pdf of the SINR gap, ν, is

$$f_\nu(y)=s\mathcal{K}|\mathbf{Z}|\,, \tag{13}$$

$$[\mathbf{Z}]_{i,j}=\begin{cases}\displaystyle\int_0^{+\infty}\phi_j(\lambda)\psi(\lambda)\,(1+\lambda)^{n_\mathrm{t}-i-1}\,\mathrm{d}\lambda & \begin{array}{l}1\le j\le n_\mathrm{t}-1\\ 1\le i\le n_\mathrm{t}-2\end{array}\\ \displaystyle\frac{1}{\delta}\int_0^{+\infty}\phi_j(\lambda)\psi(\lambda)\,(1+\lambda)\,\mathrm{e}^{-y\frac{1+\lambda}{\delta}}\,\mathrm{d}\lambda & \begin{array}{l}1\le j\le n_\mathrm{t}-1\\ i=n_\mathrm{t}-1\end{array}\end{cases} \tag{14}$$

The functions $\phi_i(\lambda)$ and $\psi(\lambda)$ have to be specified according to the adopted fading model, as detailed later. The above expression allows us to easily obtain the cdf and all moments of ν. Indeed, since integration is a linear operation, we can apply Lemma 3.1 on $\mathbf{Z}$ and get $F_\nu(y)=\int_0^y f_\nu(z)\,\mathrm{d}z=1-s\mathcal{K}|\bar{\mathbf{Z}}|$ and $m_\nu^{(k)}=s\mathcal{K}|\mathbf{Z}^{(k)}|$, where $F_\nu(y)$ is the cdf of ν, $m_\nu^{(k)}=\mathbb{E}[\nu^k]$ is the k-moment of ν,

$$[\bar{\mathbf{Z}}]_{i,j}=\begin{cases}[\mathbf{Z}]_{i,j} & \begin{array}{l}1\le j\le n_\mathrm{t}-1\\ 1\le i\le n_\mathrm{t}-2\end{array}\\ \displaystyle\int_0^{+\infty}\phi_j(\lambda)\psi(\lambda)\mathrm{e}^{-y\frac{1+\lambda}{\delta}}\,\mathrm{d}\lambda & \begin{array}{l}1\le j\le n_\mathrm{t}-1\\ i=n_\mathrm{t}-1\end{array}\end{cases}$$

$$[\mathbf{Z}^{(k)}]_{i,j}=\begin{cases}[\mathbf{Z}]_{i,j} & \begin{array}{l}1\le j\le n_\mathrm{t}-1\\ 1\le i\le n_\mathrm{t}-2\end{array}\\ \displaystyle\int_0^{+\infty}\frac{k!\delta^k\phi_j(\lambda)\psi(\lambda)}{(1+\lambda)^k}\,\mathrm{d}\lambda & \begin{array}{l}1\le j\le n_\mathrm{t}-1\\ i=n_\mathrm{t}-1\end{array}\end{cases}$$

Proof: The unconditional law of ν can be derived as:

$$f_\nu(y) = \int_{\mathbf{\Lambda}>0} f_{\nu|\mathbf{\Lambda}}(y) f_{\mathbf{\Lambda}}(\mathbf{\Lambda})\, \mathrm{d}\mathbf{\Lambda} \tag{15}$$

where $f_{\nu|\mathbf{\Lambda}}(y)$ is given by Lemma 4.1. Plugging (8) and (12) into (15), we obtain

$$f_\nu(y) = \frac{s\mathcal{K}}{(n_\mathrm{t}-1)!} \int_{\mathbf{\Lambda}>0} |\mathbf{T}||\mathbf{\Phi}| \prod_{i=1}^{n_\mathrm{t}-1} \psi(\lambda_i)\, \mathrm{d}\mathbf{\Lambda}\,. \tag{16}$$

The evaluation of the integral in (16) is carried out by resorting to Lemma 3.2. This result, specialized to our case, allows us to write:

$$\int_{\mathbf{\Lambda}>0} |\mathbf{T}||\mathbf{\Phi}| \prod_{i=1}^{n_\mathrm{t}-1} \psi(\lambda_i)\, \mathrm{d}\mathbf{\Lambda} = (n_\mathrm{t}-1)!|\mathbf{Z}|\,. \tag{17}$$

The term $(n_\mathrm{t}-1)!$ in (17) is due to the fact that now we integrate over the domain of the unordered eigenvalues $\mathbf{\Lambda}$, while in Lemma 3.2 we considered ordered variables. The elements of the matrix $\mathbf{Z}$ are given by $[\mathbf{Z}]_{i,j} = \int_0^{+\infty} t_i(\lambda)\phi_j(\lambda)\psi(\lambda)\,\mathrm{d}\lambda$. Recalling the definition of $t_i(\lambda)$ in (9), we obtain (14). ■

In the following subsections, we derive closed-form expressions for specific types of interfering fading channels, i.e., for specific expressions of the density $f_{\mathbf{\Lambda}}(\mathbf{\Lambda})$.

A. Rayleigh fading

Assume that the elements of $\widehat{\mathbf{H}}$ are zero-mean, independent, complex Gaussian random variables with unit variance and that $\widehat{\mathbf{\Delta}} = \sqrt{\hat{\delta}}\mathbf{I}$, i.e., all interfering streams have the same average power. This case well represents both the following scenarios: (i) there is a single transmitter with n_t antennas out of which one irradiates the useful signal while the others transmit interfering streams ($\delta = \hat{\delta}$); (ii) there is one transmitter with one antenna and an interfering node equipped with $n_\mathrm{t}-1$ antennas. Then the following result holds.

Proposition 4.2: The distribution of the SINR gap in (5)*, under the assumption of Rayleigh-faded interfering streams, can be written as*

$$f_\nu(y) = \frac{s\pi^2_{n_\mathrm{t}-1}}{\Gamma_{n_\mathrm{t}-1}(n_\mathrm{t}-1)\Gamma_{n_\mathrm{t}-1}(n_\mathrm{r})} |\mathbf{Z}_1|\,, \tag{18}$$

$$[\mathbf{Z}_1]_{i,j} = \begin{cases} \displaystyle\sum_{k=0}^{n_\mathrm{t}-i-1} \frac{\Gamma(n_\mathrm{r}+j-i-k)\Gamma(n_\mathrm{t}-i)}{\hat{\delta}^k k!\Gamma(n_\mathrm{t}-i-k)} & 1\le j\le n_\mathrm{t}-1 \\ & 1\le i\le n_\mathrm{t}-2 \\ \dfrac{\mathrm{e}^{-y/\delta}}{\delta}\dfrac{\tau_j!}{t^{\tau_j+1}}\left[1+\dfrac{\hat{\delta}(\tau_j+1)}{t}\right] & 1\le j\le n_\mathrm{t}-1 \\ & i=n_\mathrm{t}-1 \end{cases} \tag{19}$$

$\tau_j = n_\mathrm{r}-n_\mathrm{t}+j$, $j\in\mathbb{N}$, *and* $t = 1+\frac{\hat{\delta}}{\delta}y$.

Proof: When the columns of $\widehat{\mathbf{H}}$ are uncorrelated and Gaussian distributed, the joint pdf of the unordered eigenvalues $\mathbf{L}$ of $\widehat{\mathbf{H}}^\mathsf{H}\widehat{\mathbf{H}}$ is obtained from [27, Eq. (9)], as

$$f_{\mathbf{L}}(\mathbf{L}) = \frac{\pi^2_{n_\mathrm{t}-1}\mathcal{V}(\mathbf{L})^2 \mathrm{e}^{-\mathsf{Tr}\{\mathbf{L}\}}|\mathbf{L}|^{\tau_1}}{\Gamma_{n_\mathrm{t}-1}(n_\mathrm{t}-1)\Gamma_{n_\mathrm{t}-1}(n_\mathrm{r})(n_\mathrm{t}-1)!}\,. \tag{20}$$

Since $\widehat{\mathbf{\Delta}} = \sqrt{\hat{\delta}}\mathbf{I}$, the eigenvalues of $\mathbf{G} = \widehat{\mathbf{H}}\widehat{\mathbf{\Delta}}$ are $\mathbf{\Lambda} = \hat{\delta}\mathbf{L}$ whose distribution is

$$f_{\mathbf{\Lambda}}(\mathbf{\Lambda}) = \frac{f_{\mathbf{L}}(\mathbf{\Lambda}/\hat{\delta})}{\hat{\delta}^{n_\mathrm{t}-1}} = \frac{\pi^2_{n_\mathrm{t}-1}\mathcal{V}(\mathbf{\Lambda})^2 \mathrm{e}^{-\mathsf{Tr}\{\mathbf{\Lambda}\}/\hat{\delta}}|\mathbf{\Lambda}^{\tau_1}/\hat{\delta}^{n_\mathrm{r}}|}{\Gamma_{n_\mathrm{t}-1}(n_\mathrm{t}-1)\Gamma_{n_\mathrm{t}-1}(n_\mathrm{r})(n_\mathrm{t}-1)!}\,. \tag{21}$$

In (20) and (21), the term $(n_\mathrm{t}-1)!$ accounts for the fact that we consider unordered eigenvalues, while in [27, Eq. (9)] ordered eigenvalues were assumed.

By comparing (21) to (12), we identify the following terms: $|\mathbf{\Phi}| = \mathcal{V}(\mathbf{\Lambda})$ (i.e., $\phi_j(\lambda) = \lambda^{j-1}$), $\psi(\lambda) = \frac{1}{\hat{\delta}^{n_\mathrm{r}}}\lambda^{\tau_1}\mathrm{e}^{-\lambda/\hat{\delta}}$, and $\mathcal{K} = \frac{\pi^2_{n_\mathrm{t}-1}}{\Gamma_{n_\mathrm{t}-1}(n_\mathrm{t}-1)\Gamma_{n_\mathrm{t}-1}(n_\mathrm{r})}$ which, substituted in (14), provide

$$\begin{aligned}[\mathbf{Z}_1]_{i,j} &= \frac{1}{\hat{\delta}^{n_\mathrm{r}}}\int_0^{+\infty}(1+\lambda)^{n_\mathrm{t}-i-1}\lambda^{\tau_j}\mathrm{e}^{-\lambda/\hat{\delta}}\,\mathrm{d}\lambda \\ &= \hat{\delta}^{j-i}\sum_{k=0}^{n_\mathrm{t}-i-1}\frac{\Gamma(n_\mathrm{r}+j-i-k)\Gamma(n_\mathrm{t}-i)}{\hat{\delta}^k k!\Gamma(n_\mathrm{t}-i-k)}\end{aligned} \tag{22}$$

for $1\le i\le n_\mathrm{t}-2$ and $1\le j\le n_\mathrm{t}-1$. Instead, for $i = n_\mathrm{t}-1$,

$$\begin{aligned}[\mathbf{Z}_1]_{i,j} &= \frac{\mathrm{e}^{-y/\delta}}{\hat{\delta}^{n_\mathrm{r}}\delta}\int_0^{+\infty}(1+\lambda)\lambda^{\tau_j}\mathrm{e}^{-\lambda(1/\hat{\delta}+y/\delta)}\,\mathrm{d}\lambda \\ &= \frac{\mathrm{e}^{-y/\delta}}{\delta}\frac{\tau_j!\hat{\delta}^{j-n_\mathrm{t}+1}}{t^{\tau_j+1}}\left[1+\frac{\hat{\delta}(\tau_j+1)}{t}\right]\end{aligned} \tag{23}$$

where we recall that $\tau_j = n_\mathrm{r}-n_\mathrm{t}+j$, $j\in\mathbb{N}$, and $t = 1+\frac{\hat{\delta}}{\delta}y$. At last, observe that the determinant of a matrix $\mathbf{Z}$ such that $[\mathbf{Z}]_{i,j} = \hat{\delta}^{j-i}a_{i,j}$, equals the determinant of a matrix $\mathbf{A}$ whose (i,j)-th element is $a_{i,j}$. Thus, the factors $\hat{\delta}^{j-i}$ and $\hat{\delta}^{j-n_\mathrm{t}+1}$ can be removed from (22) and (23), respectively. ■

From the above proposition, we obtain the following interesting result on the case where the rows of $\mathbf{G}$ are correlated. Also, note that our model captures the case where interfering signals exhibit different values of path loss.

Corollary 4.1: If the rows of $\mathbf{G}$ *have zero-mean, Gaussian-distributed elements and are correlated with common covariance matrix* $\mathbf{\Sigma}$*, with distinct*[4] *eigenvalues* σ_i*,* $i = 1,\ldots,n_\mathrm{t}-1$*, the distribution of the SINR gap* ν *is given by*

$$f_\nu(y) = \frac{s\pi_{n_\mathrm{t}-1}|\mathbf{Z}_2|}{\Gamma_{n_\mathrm{t}-1}(n_\mathrm{r})\mathcal{V}(\mathbf{\Sigma})|\mathbf{\Sigma}|^{\tau_2}}, \tag{24}$$

$$[\mathbf{Z}_2]_{i,j} = \begin{cases} \displaystyle\sum_{k=0}^{n_\mathrm{t}-i-1}\frac{\Gamma(n_\mathrm{t}-i)(n_\mathrm{r}-i-k)!}{k!\Gamma(n_\mathrm{t}-i-k)\sigma_j^{k-n_\mathrm{r}+i-1}} & 1\le j\le n_\mathrm{t}-1 \\ & 1\le i\le n_\mathrm{t}-2 \\ \dfrac{\mathrm{e}^{-\frac{y}{\delta}}\tau_1!\sigma_j^{\tau_2}}{\delta(1+\frac{\sigma_j}{\delta}y)^{\tau_2}}\left(1+\dfrac{\tau_2\sigma_j}{1+\frac{\sigma_j}{\delta}y}\right) & 1\le j\le n_\mathrm{t}-1 \\ & i=n_\mathrm{t}-1 \end{cases}$$

Proof: Under the corollary's assumptions on $\mathbf{G}$, the density of $\mathbf{\Lambda}$ is given by [21, eq. (95)]:

$$f_{\mathbf{\Lambda}}(\mathbf{\Lambda}) = \pi^2_{n_\mathrm{t}-1}\frac{{}_0F_0(;;-\mathbf{\Sigma}^{-1},\mathbf{G}^\mathsf{H}\mathbf{G})|\mathbf{G}^\mathsf{H}\mathbf{G}|^{\tau_1}\mathcal{V}(\mathbf{\Lambda})^2}{(n_\mathrm{t}-1)!|\mathbf{\Sigma}|^{n_\mathrm{r}}\Gamma_{n_\mathrm{t}-1}(n_\mathrm{r})\Gamma_{n_\mathrm{t}-1}(n_\mathrm{t}-1)}\,. \tag{25}$$

In (25), the term $(n_\mathrm{t}-1)!$ is due to the fact that we consider unordered eigenvalues $\mathbf{\Lambda}$, while [21, eq. (95)] assumes ordered eigenvalues. Moreover, in (25) ${}_pF_q(\mathbf{a};\mathbf{b};\mathbf{\Phi},\mathbf{\Psi})$ is the generalized hypergeometric function of two matrix arguments. Since $|\mathbf{G}^\mathsf{H}\mathbf{G}| = |\mathbf{\Lambda}|$, $\mathcal{V}(\mathbf{G}^\mathsf{H}\mathbf{G}) = \mathcal{V}(\mathbf{\Lambda})$, ${}_0F_0(;;-\mathbf{\Sigma}^{-1},\mathbf{G}^\mathsf{H}\mathbf{G}) = \frac{\Gamma_{n_\mathrm{t}-1}(n_\mathrm{t}-1)|\mathbf{E}|}{\pi_{n_\mathrm{t}-1}\mathcal{V}(-\mathbf{\Sigma}^{-1})\mathcal{V}(\mathbf{G}^\mathsf{H}\mathbf{G})}$, $[\mathbf{E}]_{i,j} = \mathrm{e}^{-\frac{\lambda_i}{\sigma_j}}$ [27, eq. (6)], and $\mathcal{V}(-\mathbf{\Sigma}^{-1}) = \mathcal{V}(\mathbf{\Sigma})|\mathbf{\Sigma}|^{2-n_\mathrm{t}}$, the pdf of $\mathbf{\Lambda}$ can be rewritten as

$$f_{\mathbf{\Lambda}}(\mathbf{\Lambda}) = \frac{\pi_{n_\mathrm{t}-1}|\mathbf{E}||\mathbf{\Lambda}|^{\tau_1}\mathcal{V}(\mathbf{\Lambda})}{(n_\mathrm{t}-1)!\Gamma_{n_\mathrm{t}-1}(n_\mathrm{r})\mathcal{V}(\mathbf{\Sigma})|\mathbf{\Sigma}|^{\tau_2}}\,. \tag{26}$$

[4]Multiple eigenvalues can be addressed via limiting procedures [26].

By comparing (26) to (12), we identify the following terms: $\mathbf{\Phi} = \mathbf{E}$ (hence $\phi_j(\lambda_i) = \mathrm{e}^{-\lambda_i/\sigma_j}$), $\psi(\lambda) = \lambda^{\tau_1}$, and $\mathcal{K} = \frac{\pi_{n_\mathrm{t}-1}}{\Gamma_{n_\mathrm{t}-1}(n_\mathrm{r})\mathcal{V}(\mathbf{\Sigma})|\mathbf{\Sigma}|^{\tau_2}}$. By substituting these expressions in (14), after some algebra, we obtain (24). ∎

B. Rice fading

In the case of an interfering node with $n_\mathrm{t}-1$ antennas whose streams undergo Rice fading, we have $\mathbf{H} = \bar{\mathbf{H}}+\tilde{\mathbf{H}}$ where $\bar{\mathbf{H}}$ is constant and $\tilde{\mathbf{H}}$ is a random Gaussian zero-mean matrix with i.i.d. entries. This scenario is representative of a worst-case cellular transmission where the useful stream comes, e.g., from the cell edge and dominant interferers have LoS path toward the base station. We specifically consider the case where $\widehat{\mathbf{\Delta}} = \sqrt{\hat{\delta}}\mathbf{I}$ so that $\mathbf{G} = \sqrt{\hat{\delta}}\widehat{\mathbf{H}}$. Note that, in the case of r Rice-faded interferers and $n_\mathrm{t}-1-r$ Rayleigh-faded interferers, $\bar{\mathbf{H}}$ has rank less or equal to r. In the following, we provide an expression for the pdf of the SINR gap ν for a generic r by defining the matrix $\mathbf{\Omega} = \bar{\mathbf{H}}^{\mathsf{H}}\bar{\mathbf{H}}$ with rank $r \leq n_\mathrm{t}-1$. Also, we denote by $\mathbf{\Omega}_r = \mathrm{diag}(\omega_1 \ldots, \omega_r)$ the diagonal matrix containing the r distinct, non-zero eigenvalues of $\mathbf{\Omega}$.

Proposition 4.3: The distribution of the SINR gap in (5)*, under the assumption of Rice-faded interfering streams, with rank-r LoS matrix, can be written as*

$$f_\nu(y) = \frac{s\pi_{n_\mathrm{t}-1-r}\mathrm{e}^{-\mathsf{Tr}\{\mathbf{\Omega}_r\}}(\tau_1!)^{1-n_\mathrm{t}}|\mathbf{Z}_3|}{\Gamma_{n_\mathrm{t}-1-r}(n_\mathrm{t}-1-r)|\mathbf{\Omega}_r|^{n_\mathrm{t}-1-r}\mathcal{V}(\mathbf{\Omega}_r)}, \quad (27)$$

$$[\mathbf{Z}_3]_{i,j}=\begin{cases} \sum_{k=0}^{n_\mathrm{t}-i-1}\binom{n_\mathrm{t}-i-1}{k}\frac{{}_1F_1(n_\mathrm{r}-i-k+1;\tau_2;\omega_j)}{[(n_\mathrm{r}-i-k)!]^{-1}\hat{\delta}^k} & \\ \qquad 1\leq j\leq r,\ 1\leq i\leq n_\mathrm{t}-2 & \\ \sum_{k=0}^{n_\mathrm{t}-i-1}\binom{n_\mathrm{t}-i-1}{k}\frac{\tau_1!(n_\mathrm{r}+n_\mathrm{t}-i-j-k-1)!}{(n_\mathrm{r}-j)!\hat{\delta}^k} & \\ \qquad r+1\leq j\leq n_\mathrm{t}-1,\ 1\leq i\leq n_\mathrm{t}-2 & \\ \frac{\mathrm{e}^{-y/\delta}\mathrm{e}^{\omega_j/t}}{\delta}\frac{\tau_1!}{t^{\tau_3}}\left[t+\hat{\delta}\left(\tau_2+\frac{\omega_j}{t}\right)\right] & \\ \qquad 1\leq j\leq r,\ i=n_\mathrm{t}-1 & \\ \frac{\mathrm{e}^{-y/\delta}}{\delta}\frac{\tau_1!}{t^{n_\mathrm{r}-j+2}}\left[t+\hat{\delta}(n_\mathrm{r}-j+1)\right] & \\ \qquad r+1\leq j\leq n_\mathrm{t}-1,\ i=n_\mathrm{t}-1 & \end{cases}$$

Proof: The distribution of the unordered eigenvalues $\mathbf{L} = \mathrm{diag}(\ell_1, \ldots, \ell_{n_\mathrm{t}-1})$ of $\widehat{\mathbf{H}}^{\mathsf{H}}\widehat{\mathbf{H}}$ is given in [28, Eq. (46)] as:

$$f_{\mathbf{L}}(\mathbf{L})=\frac{(-1)^{\frac{r(r-1)}{2}}s\pi_{m_r}(\tau_1!)^{1-n_\mathrm{t}}|\mathbf{\Upsilon}(\mathbf{L})|\mathcal{V}(\mathbf{L})|\mathbf{L}|^{\tau_1}}{\Gamma_{m_r}(m_r)\mathrm{e}^{\mathsf{Tr}\{\mathbf{L}\}}\mathrm{e}^{\mathsf{Tr}\{\mathbf{\Omega}_r\}}|\mathbf{\Omega}_r|^{m_r}\mathcal{V}(\mathbf{\Omega}_r)(n_\mathrm{t}-1)!} \quad (28)$$

where $m_r = n_\mathrm{t}-1-r$ and [28, Formula (49)]

$$[\mathbf{\Upsilon}(\mathbf{L})]_{i,j} = \begin{cases} {}_0F_1(;\tau_2;\omega_j\ell_i), & 1\leq i\leq n_\mathrm{t}-1,\ 1\leq j\leq r \\ \frac{\ell_i^{n_\mathrm{t}-j-1}\tau_1!}{(n_\mathrm{r}-j)!}, & 1\leq i\leq n_\mathrm{t}-1,\ r+1\leq j\leq n_\mathrm{t}-1 \end{cases}$$

We remark that the term $(n_\mathrm{t}-1)!$ at the denominator of (28) accounts for the fact that we consider unordered eigenvalues, unlike in [28, Eq. (46)]. If $\widehat{\mathbf{\Delta}} = \sqrt{\hat{\delta}}\mathbf{I}$, the eigenvalues of $\mathbf{G}^{\mathsf{H}}\mathbf{G}$ are $\mathbf{\Lambda} = \hat{\delta}\mathbf{L}$ whose distribution is

$$\begin{aligned} f_{\mathbf{\Lambda}}(\mathbf{\Lambda}) &= \frac{1}{\hat{\delta}^{n_\mathrm{t}-1}}f_{\mathbf{L}}\left(\frac{\mathbf{\Lambda}}{\hat{\delta}}\right) \\ &= \frac{s\pi_{m_r}\mathrm{e}^{-\mathsf{Tr}\{\mathbf{\Omega}_r\}}(\tau_1!)^{1-n_\mathrm{t}}|\mathbf{\Upsilon}(\frac{\mathbf{\Lambda}}{\hat{\delta}})|\mathcal{V}(\mathbf{\Lambda})\left|\frac{\mathbf{\Lambda}^{\tau_1}}{\hat{\delta}^{n_\mathrm{r}-n_\mathrm{t}/2+1}}\right|}{(-1)^{\frac{r(r-1)}{2}}\mathrm{e}^{\frac{\mathsf{Tr}\{\mathbf{\Lambda}\}}{\hat{\delta}}}\Gamma_{m_r}(m_r)|\mathbf{\Omega}_r|^{m_r}\mathcal{V}(\mathbf{\Omega}_r)(n_\mathrm{t}-1)!} \end{aligned}$$

By comparing it to (12), we identify the following terms: $\mathbf{\Phi}(\mathbf{\Lambda}) = \mathbf{\Upsilon}(\frac{\mathbf{\Lambda}}{\hat{\delta}})$, i.e., $\phi_j(\lambda_i) = [\mathbf{\Upsilon}(\frac{\mathbf{\Lambda}}{\hat{\delta}})]_{i,j}$, $\psi(\lambda) = \frac{\lambda^{\tau_1}\mathrm{e}^{-\lambda/\hat{\delta}}}{\hat{\delta}^{n_\mathrm{r}-n_\mathrm{t}/2+1}}$, and $\mathcal{K} = \frac{(-1)^{r(r-1)/2}s\pi_{m_r}(\tau_1!)^{1-n_\mathrm{t}}}{\mathrm{e}^{\mathsf{Tr}\{\mathbf{\Omega}_r\}}\Gamma_{m_r}(m_r)|\mathbf{\Omega}_r|^{m_r}\mathcal{V}(\mathbf{\Omega}_r)}$. The integral in (14) is then solved by exploiting the following formula

$$\int_0^{+\infty}{}_0F_1\left(;b;\frac{\omega}{\hat{\delta}}\lambda\right)\lambda^m\mathrm{e}^{-\theta\lambda}\,\mathrm{d}\lambda=\frac{\Gamma(m+1)}{\theta^{m+1}}{}_1F_1\left(m+1;b;\frac{\omega}{\hat{\delta}\theta}\right),$$

$\theta > 0$. After some algebra, we obtain (27). ∎

The corollary below refers to a full-rank LoS matrix $\mathbf{\Omega}$ with equal eigenvalues. This case, initially considered in [29], represents an optimized LoS MIMO system where the correlation between the LoS responses is removed, thereby resulting in orthogonal spatial LoS subchannels.

Corollary 4.2: When $r = n_\mathrm{t}-1$ and $\omega_i = \omega$, $i = 1, \ldots, n_\mathrm{t}-1$, the distribution of the SINR gap in Proposition 4.3 reduces to

$$f_\nu(y) = \frac{s\pi_{n_\mathrm{t}-1}\mathrm{e}^{-\omega(n_\mathrm{t}-1)}|\mathbf{Z}_4|}{\Gamma_{n_\mathrm{t}-1}(n_\mathrm{t}-1)},$$

$$[\mathbf{Z}_4]_{i,j}=\begin{cases} \sum_{k=0}^{n_\mathrm{t}-i-1}\binom{n_\mathrm{t}-i-1}{k}\frac{\Gamma(\varphi){}_1F_1(\varphi;n_\mathrm{r}-j+1;\omega)}{(n_\mathrm{r}-j)!\hat{\delta}^k} & \\ \qquad 1\leq j\leq n_\mathrm{t}-1,\ 1\leq i\leq n_\mathrm{t}-2 & \\ \frac{\mathrm{e}^{-y/\delta+\frac{\omega}{t}}}{\delta t^{n_\mathrm{r}-j+2}}\left[t+\hat{\delta}\left(n_\mathrm{r}-j+1+\frac{\omega}{t}\right)\right] & \\ \qquad 1\leq j\leq n_\mathrm{t}-1,\ i=n_\mathrm{t}-1 & \end{cases}$$

and $\varphi = n_\mathrm{r}+n_\mathrm{t}-i-j-k$.

Proof: If the LoS channel matrix $\widehat{\mathbf{H}}$ is full rank and has all-equal eigenvalues, the density of the unordered eigenvalues of $\widehat{\mathbf{H}}^{\mathsf{H}}\widehat{\mathbf{H}}$, $f(\mathbf{L})$, is given by [29, Eq. (6)], i.e.,

$$f_{\mathbf{L}}(\mathbf{L}) = \frac{s\pi_{n_\mathrm{t}-1}\mathrm{e}^{-\omega(n_\mathrm{t}-1)}|\mathbf{\Upsilon}_1(\mathbf{L})|\mathcal{V}(\mathbf{L})|\mathbf{L}|^{\tau_1}}{\mathrm{e}^{\mathsf{Tr}\{\mathbf{L}\}}\Gamma_{n_\mathrm{t}-1}(n_\mathrm{t}-1)(n_\mathrm{t}-1)!},$$

with $[\mathbf{\Upsilon}_1]_{i,j} = \frac{\ell_i^{n_\mathrm{t}-j-1}}{(n_\mathrm{r}-j)!}{}_0F_1(;n_\mathrm{r}-j+1;\omega\ell_i)$. When $\widehat{\mathbf{\Delta}} = \sqrt{\hat{\delta}}\mathbf{I}$, $\mathbf{\Lambda} = \hat{\delta}\mathbf{L}$ has density

$$f_{\mathbf{\Lambda}}(\mathbf{\Lambda}) = \frac{s\pi_{n_\mathrm{t}-1}|\mathbf{\Upsilon}_1(\frac{\mathbf{\Lambda}}{\hat{\delta}})|\mathcal{V}(\mathbf{\Lambda})\left|\frac{\mathbf{\Lambda}^{\tau_1}}{\hat{\delta}^{n_\mathrm{r}-n_\mathrm{t}/2+1}}\right|}{\mathrm{e}^{\omega(n_\mathrm{t}-1)}\mathrm{e}^{\frac{\mathsf{Tr}\{\mathbf{\Lambda}\}}{\hat{\delta}}}\Gamma_{n_\mathrm{t}-1}(n_\mathrm{t}-1)(n_\mathrm{t}-1)!} \quad (29)$$

By comparing (29) to (12), we identify $\phi_j(\lambda_i) = [\mathbf{\Upsilon}_1(\frac{\mathbf{\Lambda}}{\hat{\delta}})]_{i,j}$, $\psi(\lambda) = \frac{\lambda^{\tau_1}\mathrm{e}^{-\lambda/\hat{\delta}}}{\hat{\delta}^{n_\mathrm{r}-n_\mathrm{t}/2+1}}$, and $\mathcal{K} = s\frac{\pi_{n_\mathrm{t}-1}\mathrm{e}^{-\omega(n_\mathrm{t}-1)}}{\Gamma_{n_\mathrm{t}-1}(n_\mathrm{t}-1)}$. The matrix $\mathbf{Z}_4$ is then obtained by computing (14). ∎

C. Small-cells and multiple scattering

Finally, we consider the case where there is an interfering node equipped with $n_\mathrm{t}-1$ antennas and all streams undergo a multiple-scattering channel with $N-1$ clusters of n_i independent scatterers each. This scenario is of particular interest in small-cells networks. Indeed, it adequately represents, with no

approximation in the channel statistics, the case where interfering signals come from non co-located single-antenna equipped users, whose signals may undergo multiple scattering.

In this case, $\widehat{\mathbf{H}}$ can be represented by the product of N matrices, $\mathbf{K}_i$, of size $n_i \times n_{i-1}$, $i=1,\ldots,N$, with $n_0 = n_\mathrm{t}-1$ and $n_N = n_\mathrm{r}$. The entries of $\mathbf{K}_i$ are zero-mean unit variance, complex Gaussian, independent random variables. For compactness, we define the set of auxiliary variables $\zeta_i = n_i - n_0$, $i=1,\ldots,N$. Also, we assume $n_\mathrm{t}-1 \le n_1 \le \ldots \le n_\mathrm{r}$, thus the variables ζ_i are non-negative integers.

Proposition 4.4: The distribution of the SINR gap in (5)*, under the assumption of multiple Rayleigh scattering affecting the interfering streams, can be written as*

$$f_\nu(y) = \frac{s|\mathbf{Z}_5|}{\prod_{i=1}^{n_0}\prod_{\ell=0}^{N}\Gamma(i+\zeta_\ell)}, \tag{30}$$

$$[\mathbf{Z}_5]_{i,j} = \begin{cases} \displaystyle\sum_{k=0}^{n_\mathrm{t}-i-1}\binom{n_\mathrm{t}-i-1}{k}\frac{\Gamma(n_1+j-i-k)}{\hat{\delta}^k}\prod_{q=2}^{N}(n_q-i-\ell)! \\ \qquad\qquad 1\le j\le n_\mathrm{t}-1,\ 1\le i\le n_\mathrm{t}-2 \\ \dfrac{\mathrm{e}^{-\frac{y}{\hat{\delta}}}}{\hat{\delta}y}\left[G_{1,N}^{N,1}\left(\begin{matrix}0\\ \boldsymbol{\zeta}_j\end{matrix}\middle|\frac{\delta}{\hat{\delta}y}\right)+\frac{\delta}{y}G_{1,N}^{N,1}\left(\begin{matrix}-1\\ \boldsymbol{\zeta}_j\end{matrix}\middle|\frac{\delta}{\hat{\delta}y}\right)\right] \\ \qquad\qquad 1\le j\le n_\mathrm{t}-1,\ i=n_\mathrm{t}-1 \end{cases}$$

and $\boldsymbol{\zeta}_j = [\zeta_N,\ldots,\zeta_2,\zeta_1+j-1]$.

Proof: The density of the unordered eigenvalues $\mathbf{L}$ of $\widehat{\mathbf{H}}^\mathsf{H}\widehat{\mathbf{H}}$ is given by [30, Eq. (8)]:

$$f_\mathbf{L}(\mathbf{L}) = \frac{\mathcal{V}(\mathbf{L})|\boldsymbol{\Gamma}(\mathbf{L})|}{n_0!\prod_{i=1}^{n_0}\prod_{\ell=0}^{N}\Gamma(i+\zeta_\ell)}, \tag{31}$$

where $\boldsymbol{\Gamma}(\mathbf{L})$ is an $n_0\times n_0$ matrix with entries $[\boldsymbol{\Gamma}(\mathbf{L})]_{i,j} = G_{0,N}^{N,0}\left(\begin{matrix}-\\ \boldsymbol{\zeta}_j\end{matrix}\middle|\ell_i\right)$, for $i,j=1,\ldots,n_0$. When $\widehat{\boldsymbol{\Delta}} = \sqrt{\hat{\delta}}\mathbf{I}$, the density of the unordered eigenvalues $\boldsymbol{\Lambda} = \hat{\delta}\mathbf{L}$ of $\mathbf{G}^\mathsf{H}\mathbf{G}$ is

$$f_{\boldsymbol{\Lambda}}(\boldsymbol{\Lambda}) = \frac{\mathcal{V}(\boldsymbol{\Lambda})|\boldsymbol{\Gamma}(\boldsymbol{\Lambda}/\hat{\delta})|}{\hat{\delta}^{(n_\mathrm{t}-1)n_\mathrm{t}/2}n_0!\prod_{i=1}^{n_0}\prod_{\ell=0}^{N}\Gamma(i+\zeta_\ell)}. \tag{32}$$

Comparing (32) to (12), we identify $\phi_j(\lambda_i)=[\boldsymbol{\Gamma}(\boldsymbol{\Lambda}/\hat{\delta})]_{i,j}$, $\psi(\lambda)=\hat{\delta}^{-(n_\mathrm{t}-1)n_\mathrm{t}/2}$, and $\mathcal{K}=\frac{1}{\prod_{i=1}^{n_0}\prod_{\ell=0}^{N}\Gamma(i+\zeta_\ell)}$. We proceed along the lines of previous proofs. The evaluation of (14), for $1\le i\le n_\mathrm{t}-2$ and $1\le j\le n_\mathrm{t}-1$, can be carried out by exploiting the expression [20, 7.811.4], which provides integrals of the type $\int_0^{+\infty}\lambda^n G_{a,b}^{c,d}(\cdot|\theta\lambda)\,\mathrm{d}\lambda$. Instead, for $i=n_\mathrm{t}-1$ and $1\le j\le n_\mathrm{t}-1$, the evaluation of (14) can be carried out by using [20, 7.813.1], which provides the expression of integrals of the type $\int_0^{+\infty}\lambda^{-n}\mathrm{e}^{-\lambda}G_{a,b}^{c,d}(\cdot|\theta\lambda)\,\mathrm{d}\lambda$. ■

V. Applications of the SINR Gap Statistics

Here we present two main applications of the SINR gap statistics evaluation, focusing on the symbol error rate and the outage probability.

A. Symbol error rate achieved by the ZF and MMSE receivers

In the presence of an M-PSK-modulated input signal and by modeling the SINR with the random variable γ, the achieved symbol error rate can be expressed as [14, eq.(5)] $P_e = \frac{1}{\pi}\int_0^\Theta \mathcal{M}_\gamma\left(-\frac{c}{\sin^2\theta}\right)\mathrm{d}\theta$ where $c=\sin^2(\pi/M)$, $\mathcal{M}_\gamma(s) = \mathbb{E}_\gamma[\mathrm{e}^{s\gamma}]$ is the moment generating function of the SINR, and $\Theta = \pi\frac{M-1}{M}$. Such an expression for P_e is difficult to evaluate, due to the integration with respect to θ. To overcome this problem, the following approximation to P_e has been proposed in [14, eq.(10)], which proved to be very accurate:

$$\begin{aligned} P_e \;\approx\; & \left(\frac{\Theta}{2\pi}-\frac{1}{6}\right)\mathcal{M}_\gamma(-c)+\frac{1}{4}\mathcal{M}_\gamma\left(-\frac{4c}{3}\right) \\ & +\left(\frac{\Theta}{2\pi}-\frac{1}{4}\right)\mathcal{M}_\gamma\left(-\frac{c}{\sin^2\Theta}\right). \end{aligned} \tag{33}$$

We now investigate the case where the MMSE filter is employed to process the intended stream, thus $\gamma=\gamma^\mathrm{mmse} = \gamma^\mathrm{zf}+\nu$. When the random variables γ^zf and ν are independent, the moment generating function of the SINR γ^mmse factorizes as $\mathcal{M}_{\gamma^\mathrm{mmse}}(s) = \mathcal{M}_{\gamma^\mathrm{zf}}(s)\mathcal{M}_\nu(s)$. Note that, as proven in [2, Th. III.1], the independence between γ^zf and ν holds true when the Rayleigh-faded useful signal is subject to independent Rayleigh-faded interferers, i.e., when the vector $\mathbf{h}$ and the columns of the matrix $\mathbf{G} = \mathbf{U}\boldsymbol{\Lambda}^{1/2}\mathbf{V}^\mathsf{H}$ are Gaussian and independent. Interestingly, the result applies also to any unitarily invariant matrix $\mathbf{G}$ since the proof of [2, Th. III.1] exploits the independence between $\boldsymbol{\Lambda}$ and $\mathbf{U}$, which holds for all unitarily invariant matrices.

By exploiting the expression of the density of ν in (13), the moment generating function $\mathcal{M}_\nu(s)$ can be written as

$$\mathcal{M}_\nu(s) = s\mathcal{K}|\mathbf{M}|, \tag{34}$$

$$[\mathbf{M}]_{i,j} = \begin{cases} [\mathbf{Z}]_{i,j} & 1\le j\le n_\mathrm{t}-1,\ 1\le i\le n_\mathrm{t}-2 \\ \int_0^\infty \mathrm{e}^{sy}[\mathbf{Z}]_{i,j}\,\mathrm{d}y & 1\le j\le n_\mathrm{t}-1,\ i=n_\mathrm{t}-1 \end{cases}$$

Remark I: The result in (34) is obtained by applying Lemma 3.1 and by observing that $\mathbb{E}_\gamma[\cdot]$ is a linear operator. For example, in the case of Rayleigh interferers, we have $\mathcal{M}_\nu(s) = \frac{s\pi_{n_\mathrm{t}-1}^2}{\Gamma_{n_\mathrm{t}-1}(n_\mathrm{t}-1)\Gamma_{n_\mathrm{t}-1}(n_\mathrm{r})}|\mathbf{M}_1|$ with

$$[\mathbf{M}_1]_{i,j} = \begin{cases} \displaystyle\sum_{k=0}^{n_\mathrm{t}-i-1}\frac{\Gamma(n_\mathrm{r}+j-i-k)\Gamma(n_\mathrm{t}-i)}{\hat{\delta}^k k!\Gamma(n_\mathrm{t}-i-k)} \\ \qquad\qquad 1\le j\le n_\mathrm{t}-1,\ 1\le i\le n_\mathrm{t}-2 \\ \mathrm{e}^{\hat{s}}\tau_j!\left[\dfrac{1}{\hat{\delta}}\mathrm{Ei}\left(\tau_j+1,\hat{s}\right)+(\tau_j+1)\mathrm{Ei}\left(\tau_j+2,\hat{s}\right)\right] \\ \qquad\qquad 1\le j\le n_\mathrm{t}-1,\ i=n_\mathrm{t}-1 \end{cases}$$

where $\hat{s}=\frac{1-s\delta}{\hat{\delta}}$ and $\mathrm{Ei}(\cdot,\cdot)$ is the generalized exponential integral. The expression of γ^zf is reported in (1) and can be rewritten as [2, eq. (15)] $\gamma^\mathrm{zf} = \delta\rho$, where $\rho = \mathbf{h}^\mathsf{H}\left[\mathbf{I}-\mathbf{G}(\mathbf{G}^\mathsf{H}\mathbf{G})^{-1}\mathbf{G}^\mathsf{H}\right]\mathbf{h}$. Given the density of ρ, $f_\rho(z) = \frac{z^{n_\mathrm{r}-n_\mathrm{t}}}{(n_\mathrm{r}-n_\mathrm{t})!}\mathrm{e}^{-z}$ [2, eq. (16)], we get the density of γ^zf as $f_{\gamma^\mathrm{zf}}(z) = \frac{1}{\delta}f_\rho\left(\frac{z}{\delta}\right)$. Hence, $\mathcal{M}_{\gamma^\mathrm{zf}}(s) = (1-s\delta)^{-(n_\mathrm{r}-n_\mathrm{t}+1)}$, from which the symbol error rate can be easily obtained.

B. Outage probability

Let us now assume that the useful stream is coded with rate R, then its outage probability when the MMSE receiver is employed is given by $P_{\rm out}^{\rm mmse}(R)=\mathbb{P}\left(\log(1+\gamma^{\rm mmse})<R\right)$. By using the definition of the SINR gap in (2), we can rewrite $P_{\rm out}^{\rm mmse}$ as a function of the SINR gap ν and of the outage probability achieved by the ZF receiver, $P_{\rm out}^{\rm zf}(R)$, i.e.,

$$P_{\rm out}^{\rm mmse}(R)=\mathbb{P}\left(\log(1+\gamma^{\rm zf}+\nu)<R\right)=\mathbb{P}\left(\gamma^{\rm zf}<2^R-1-\nu\right)\,.$$

As mentioned in the previous section, $\gamma^{\rm zf}=\delta\rho$ and, under the assumption of unitarily invariant matrix $\mathbf{G}$, we have:

$$P_{\rm out}^{\rm mmse}(R)=\mathbb{P}\left(\rho<\frac{2^R-1-\nu}{\delta}\right)=\int_0^{2^R-1}F_\rho\left(\frac{2^R-1-y}{\delta}\right)f_\nu(y)\,{\rm d}y$$

where $F_\rho(\cdot)$ is the cumulative distribution function of ρ.

When the distribution of the SINR gap takes the form in (13), by Lemma 3.1, the outage probability becomes

$$P_{\rm out}^{\rm mmse}(R)=s\mathcal{K}|\mathbf{O}|, \tag{35}$$

$$[\mathbf{O}]_{i,j}=\begin{cases}[\mathbf{Z}]_{i,j} & \begin{array}{l}1\le j\le n_{\rm t}-1\\ 1\le i\le n_{\rm t}-2\end{array}\\ \displaystyle\int_0^{2^R-1}F_\rho\left(\frac{2^R-1-y}{\delta}\right)[\mathbf{Z}]_{n_{\rm t}-1,j}\,{\rm d}y & \begin{array}{l}1\le j\le n_{\rm t}-1\\ i=n_{\rm t}-1\end{array}\end{cases}$$

We now consider the case where all interfering streams are affected by Rayleigh fading. Then the following holds.

Proposition 5.1: In the case of independent Rayleigh-faded interfering streams and $\widehat{\mathbf{\Delta}}=\sqrt{\hat\delta}\mathbf{I}$, the outage probability can be expressed as $P_{\rm out}^{\rm mmse}(R)=\frac{s\pi_{n_{\rm t}-1}^2}{\Gamma_{n_{\rm t}-1}(n_{\rm t}-1)\Gamma_{n_{\rm t}-1}(n_{\rm r})}|\mathbf{O}_1|$ where

$$[\mathbf{O}_1]_{i,j}=\begin{cases}\displaystyle\sum_{k=0}^{n_{\rm t}-i-1}\frac{\Gamma(n_{\rm r}+j-i-k)\Gamma(n_{\rm t}-i)}{\hat\delta^k k!\Gamma(n_{\rm t}-i-k)} & \\ \qquad 1\le j\le n_{\rm t}-1,\ 1\le i\le n_{\rm t}-2 & \\ \tau_j!\left(1-\dfrac{{\rm e}^{-\frac{u}{\delta}}}{(\frac{\hat\delta}{\delta}u+1)^{\tau_j+1}}\right) & \\ \displaystyle-\frac{\tau_j!}{{\rm e}^{\frac{u}{\delta}}}\sum_{\ell=0}^{n_{\rm r}-n_{\rm t}}\frac{u^{\ell+1}\left[\zeta_{\tau_j+1}+\hat\delta(\tau_j+1)\zeta_{\tau_j+2}\right]}{(\ell+1)!\delta^{\ell+1}} & \\ \qquad 1\le j\le n_{\rm t}-1,\ i=n_{\rm t}-1 & \end{cases}$$

$\zeta_p={}_2F_1\left(1,p;\ell+2;-\frac{\hat\delta}{\delta}u\right)$ *and* $u=2^R-1$.

Proof: In the case of independent Rayleigh-faded interfering streams, the density and the cdf of ρ are given by, respectively, $f_\rho(z)=\frac{z^{n_{\rm r}-n_{\rm t}}}{(n_{\rm r}-n_{\rm t})!}{\rm e}^{-z}$ and $F_\rho(z)=1-{\rm e}^{-z}\sum_{\ell=0}^{n_{\rm r}-n_{\rm t}}\frac{z^\ell}{\ell!}$, while the pdf of ν is given in (18). Therefore, by using the expression for $F_\rho(z)$ and the result in (19), the integral in (35) becomes $[\mathbf{O}_1]_{n_{\rm t}-1,j}=a_j-{\rm e}^{-u/\delta}\tau_j!\sum_{\ell=0}^{n_{\rm r}-n_{\rm t}}\frac{b_{j,\ell}}{\ell!\delta^{\ell+1}}$ where

$$\begin{aligned}a_j &= \frac{\tau_j!}{\delta}\int_0^u\frac{{\rm e}^{-y/\delta}}{t^{\tau_j+1}}\left(1+\frac{\hat\delta(\tau_j+1)}{t}\right){\rm d}y\,,\\ b_{j,\ell} &= \int_0^u\frac{(u-y)^\ell}{t^{\tau_j+1}}\left(1+\frac{\hat\delta(\tau_j+1)}{t}\right){\rm d}y\,,\end{aligned}$$

$u=2^R-1$, and where we recall that $\tau_j=n_{\rm r}-n_{\rm t}+j$. By applying the change of variable $x=\frac{\hat\delta}{\delta}y$, a_j can be rewritten as

$$a_j = \tau_j!\int_0^w\frac{{\rm e}^{-x/\hat\delta}}{(1+x)^{\tau_j+1}}\left(\frac{1}{\hat\delta}+\frac{\tau_j+1}{1+x}\right){\rm d}x$$

where $w=\frac{\hat\delta}{\delta}u$. To solve the above integral, we can use a special case of the expression reported in [20, 3.353.1], i.e.,

$$\begin{aligned}\int_w^\infty\frac{{\rm e}^{-x/\hat\delta}}{(1+x)^h}\,{\rm d}x &= {\rm e}^{-w/\hat\delta}\sum_{k=1}^{h-1}\frac{\Gamma(k)(-\hat\delta)^{1+k-h}}{\Gamma(h)(w+1)^k}\\ &\quad-\frac{{\rm e}^{1/\hat\delta}(-\hat\delta)^{1-h}}{\Gamma(h)}{\rm Ei}\left[-\frac{w+1}{\hat\delta}\right]\end{aligned}$$

Let $q(x)={\rm e}^{-\frac{x}{\hat\delta}}\left(1+\frac{\hat\delta(\tau_j+1)}{1+x}\right)(1+x)^{-\tau_j-1}$. After some algebra, we obtain $\int_w^\infty q(x)\,{\rm d}x=\frac{\hat\delta{\rm e}^{-\frac{w}{\hat\delta}}}{(w+1)^{\tau_j+1}}$ which, for $w=0$, provides $\int_0^\infty q(x)\,{\rm d}x=\hat\delta$. In conclusion, $a_j=\tau_j!\left(1-\frac{{\rm e}^{-w/\hat\delta}}{(w+1)^{\tau_j+1}}\right)$. To solve the integral in $b_{j,\ell}$, we can resort to a particular case of [20, 3.196.1], i.e.,

$$\int_0^w\frac{(w-x)^\ell}{(1+x)^h}\,{\rm d}x=\frac{w^{\ell+1}}{\ell+1}{}_2F_1\left(1,h;\ell+2;-w\right)$$

and, defining $\hat J(p)={}_2F_1\left(1,p;\ell+2;-w\right)$, we obtain

$$\begin{aligned}b_{j,\ell} &= \int_0^u\frac{(u-y)^\ell}{t^{\tau_j+1}}\left(1+\frac{\hat\delta(\tau_j+1)}{t}\right){\rm d}y\\ &= \frac{u^{\ell+1}}{\ell+1}\left[J(\tau_j+1)+\hat\delta(\tau_j+1)J(\tau_j+2)\right]\,.\end{aligned}$$

■

Notably, similar results can be derived for Rice interfering streams for both rank 1 and full rank matrices $\mathbf{\Omega}$, using the distributions of ρ in [9, Eq. (51)] and [9, Eq. (53)], respectively.

VI. Numerical results on the SINR gap

We now validate our analytical expressions for the pdf of the SINR gap ν, against Monte Carlo simulations. The excellent match between the two sets of results is shown in Fig. 2(left) where solid lines have been obtained by evaluating the analytical expressions in (18), (27), and (30), and refer to, respectively, Rayleigh, Rice, and multiscattering distributed interfering channels. Markers, instead, refer to the numerical results obtained by randomly generating 10^6 outcomes of the random variable ν. As for the system parameters, we set $\hat\delta=1$, $n_{\rm r}=6$, $n_{\rm t}=4$; also, we set $\delta=2$ in the Rayleigh case, and $\delta=5$, $r=1$, and $[\bar{\mathbf{H}}]_{1,j}=j$, $j=1,\ldots,n_{\rm r}$ and $[\bar{\mathbf{H}}]_{i,j}=0$ $\forall i\neq 1$, for the Rice case. For the multiscattering channel, we considered one cluster of scatterers with $n_0=3$, $n_1=5$, $n_2=6$, and $\delta=10$.

Fig. 2(right) shows the evolution of the pdf of the SINR gap as the SNR δ varies, and when the interfering streams are subject to Rayleigh channel, $n_{\rm r}=n_{\rm t}=4$, and $\hat\delta=\delta$ (i.e., the power of the useful signal and that of the interfering streams increase at the same pace). We observe that, as the SNR grows, the SINR gap does not vanish. On the contrary, it asymptotically tends to a limit distribution, as already noted in [2]. Specifically, for $\hat\delta=\delta$ and Rayleigh-distributed interferers, as $\delta\to\infty$, $f_\nu(y)$ tends to the Fisher-Snedecor distribution (or F-distribution) [2, eq.(4)]. We point out, however, that our analytical results hold also in the finite SNR regime, thus representing a more general characterization of the SINR gap. Such a characterization can be used in the

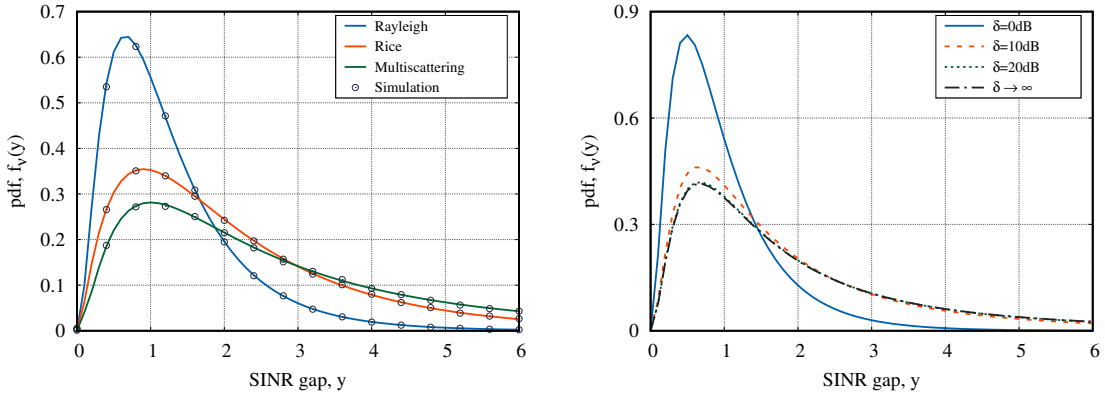

Fig. 2. Pdf of the SINR gap. Left: Numerical simulations vs. analysis for Rayleigh, Rice, and multiscattering distributed interferer channel. Right: Analytical results as functions of the SNR δ, under Rayleigh distributed interferer channel and for $n_{\rm r} = n_{\rm t} = 4$, and $\hat{\delta} = \delta$.

asymptotic case as well as for any arbitrary value of the ratio $\hat{\delta}/\delta$, in the case of Rayleigh interferers as well as in the case of other distributions of the interfering channels.

As an example, Fig. 3(left) depicts the evolution of the SINR gap as the SNR δ grows, for $\hat{\delta}/\delta = 10$, $n_{\rm r} = 6$, $n_{\rm t} = 4$, and Rice-distributed interferers characterized by $[\bar{\mathbf{H}}]_{1,j} = j/n_{\rm r}$, $j = 1, \ldots, n_{\rm r}$ and $[\bar{\mathbf{H}}]_{i,j} = 0$ for $i \neq 1$. Even in this case, we observe that the distribution of the SINR gap tends to a limit distribution whose expression (omitted for space limitations), can be readily obtained from (27) by letting δ tend to infinity with constant ratio $\hat{\delta}/\delta$.

Fig. 3(right) shows the evolution of the pdf of the SINR gap as the number of transmit ($n_{\rm t}$) and receive ($n_{\rm r}$) antennas varies, for a fixed ratio $n_{\rm t}/n_{\rm r} = 2/3$, $\delta = 10$, and $\hat{\delta} = 1$. The interferers are Rice distributed and the entries of the matrix $[\bar{\mathbf{H}}]$ are as in Fig. 3(left). Again, we observe the perfect match between Monte Carlo simulation and analytical results. Moreover, as $n_{\rm t}$ increases, the distribution of the SNR gap shifts to the right. This behavior is due to the fact that the power of the interferers grows as the number of interfering antennas ($n_{\rm t}-1$) increases, and that higher interference results in a larger performance gap between MMSE and ZF receivers.

As an application of the results obtained in Sec. IV, Fig. 4(left) shows the symbol error probability, when the transmitters send M-PSK modulated signals, the receiver employs the MMSE filter, and the interferers are subject to Rayleigh fading. The curves show the approximation in (33) for $M = 2, 4, 8$ and $\hat{\delta} = 1$, versus the SNR δ. Instead, points represent the results obtained via Monte Carlo simulations of the transmitter-receiver chain. These results not only confirm the validity of our analysis, but they also underline the importance of having exact expressions available for the SINR gap, in order to assess the system performance.

Finally, Fig. 4(right) shows the outage probability achieved by the MMSE receiver (obtained by computing (35)), as a function of the SNR δ. Results refer to the case of Rayleigh distributed interferer channels, $n_{\rm r} = 8$, $\hat{\delta} = 1$, $R = 1$, and different values of the number of transmit antennas. We observe that, since the interference level increases with the number of interfering streams (i.e., $n_{\rm t} - 1$), so does the outage probability. Conversely, if the number of interferers is kept constant, a larger number of receive antennas lead to a lower outage probability. Interestingly, the curve for $n_r = 6$ and $n_t = 5$ coincides with that experimentally obtained by simulation in [2]. As mentioned, however, all our results in Fig. 4(right) have been derived using the closed-form expressions in Proposition 5.1.

VII. Statistical Characterization of the ME Gap

This section is devoted to the derivation of the closed-form expressions of the pdf and cdf of the ME gap μ, defined in (6). Hereinafter, we present such derivation for $n_{\rm r} \geq n_{\rm t}$. We point out that the cases $n_{\rm r} = n_{\rm t}$ and $n_{\rm r} > n_{\rm t}$ correspond, respectively, to the absence and to the presence of multiple zero-eigenvalues in the matrix $\mathbf{A}$.

We first present our result under general assumptions on the fading affecting the interfering streams, then we detail the analysis under specific fading assumptions. Note that also the expression of the ME gap distribution turns out to be the product of a constant by a matrix determinant. We prove such result by leveraging results on the Rayleigh quotient.

Proposition 7.1: Let us consider the ME gap μ in (6) *where $\mathbf{A}$ is a Hermitian random matrix with non-zero eigenvalues $\alpha_1, \ldots, \alpha_{n_{\rm t}-1}$, $\alpha_i = (1+\lambda_i)^{-1}$ depending on the eigenvalues $\lambda_1, \ldots, \lambda_{n_{\rm t}-1}$ of the interfering matrix $\mathbf{G}^{\rm H}\mathbf{G}$. Assume that $\mathbf{h}$ is a standard complex Gaussian vector of size $n_{\rm r}$ with uncorrelated entries and that the joint law of the $n_{\rm t}-1$ (distinct) non-zero, unordered, positive eigenvalues $\mathbf{\Lambda}$ of $\mathbf{G}^{\rm H}\mathbf{G}$, can be written as in* (12)*. Then, the cdf and the pdf of μ admit the following closed-form expressions, respectively,*

$$F_\mu(y) = 1 - \mathcal{K}|\bar{\mathbf{Q}}|, \qquad f_\mu(y) = \mathcal{K}|\mathbf{Q}|, \tag{36}$$

$$[\bar{\mathbf{Q}}]_{i,j} = \begin{cases} \mathcal{I}_{j,n_{\rm r}-1}(y) & i = 1 \\ & 1 \leq j \leq n_{\rm t}-1 \\ \displaystyle\int_0^\infty \lambda^{i-2}\phi_j(\lambda)\psi(\lambda)(1+\lambda)\,{\rm d}\lambda & 2 \leq i \leq n_{\rm t}-1 \\ & 1 \leq j \leq n_{\rm t}-1 \end{cases}$$

$$[\mathbf{Q}]_{i,j} = \begin{cases} (n_{\rm r}-1)\mathcal{I}_{j,n_{\rm r}-2}(y) & i = 1 \\ & 1 \leq j \leq n_{\rm t}-1 \\ [\bar{\mathbf{Q}}]_{i,j} & 2 \leq i \leq n_{\rm t}-1 \\ & 1 \leq j \leq n_{\rm t}-1 \end{cases} \tag{37}$$

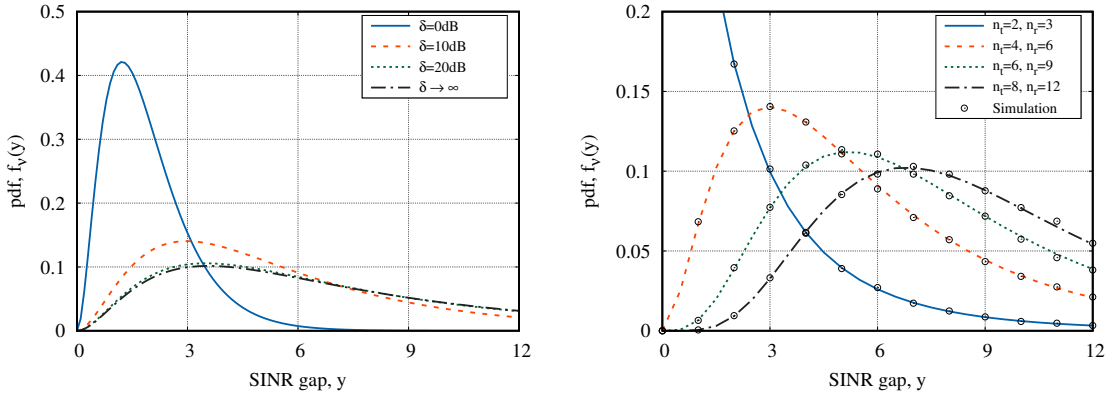

Fig. 3. Pdf of the SINR gap in the case of Rice-distributed interferers. Left: results as the SNR δ varies and for $\delta/\hat{\delta} = 10$, $n_\mathrm{r} = 6$, $n_\mathrm{t} = 4$, and $[\bar{\mathbf{H}}]_{1,j} = j/n_\mathrm{r}$, $j = 1, \ldots, n_\mathrm{r}$ and $[\bar{\mathbf{H}}]_{i,j} = 0$ for $i \neq 1$. Right: results as the number of antennas varies, for $\delta = 10$, $\hat{\delta} = 1$, $[\bar{\mathbf{H}}]_{1,j} = j/n_\mathrm{r}$, $j = 1, \ldots, n_\mathrm{r}$, and $[\bar{\mathbf{H}}]_{i,j} = 0$ for $i \neq 1$.

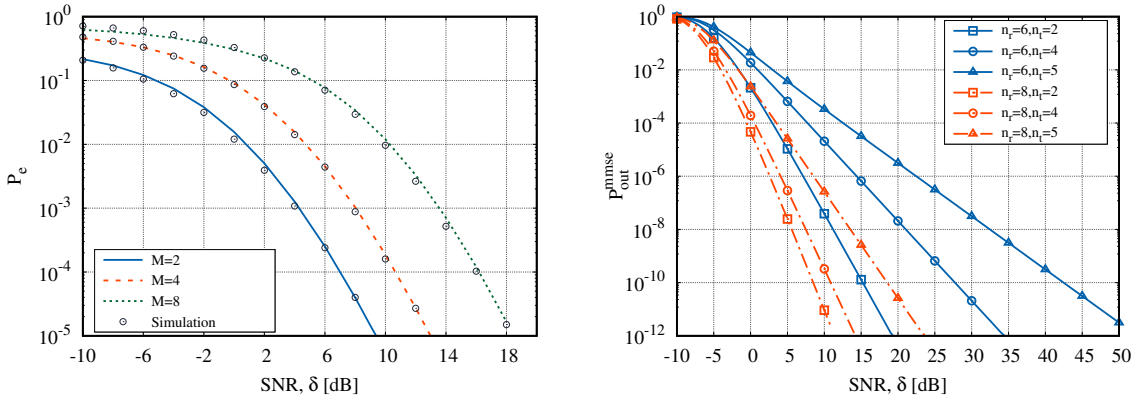

Fig. 4. Left: Symbol error probability achieved by the MMSE filter plotted versus the SNR δ, for M-PSK modulations with $M = 2, 4, 8$ and $\hat{\delta} = 1$. Lines refer to the approximation in (33), points refer to the Monte Carlo simulation. Right: Outage probability achieved by the MMSE receiver versus the SNR δ, as the number of transmit antennas varies, in the case of Rayleigh-distributed interferer channel, $n_\mathrm{r} = 8$, $\hat{\delta} = 1$, and $R = 1$.

and, defining $v = \frac{1-y}{y}$,

$$\mathcal{I}_{j,q}(y) = y^q \int_0^v (v-\lambda)^q (1+\lambda)^{n_\mathrm{r}-1-q} \phi_j(\lambda)\psi(\lambda)\,\mathrm{d}\lambda\,. \quad (38)$$

Proof: The proof is organized in two parts. First, we derive the expression of the conditional distribution $F_{\mu|\mathbf{\Lambda}}(y)$, then we consider the randomness of the eigenvalues, $\mathbf{\Lambda}$, and compute the average $F_\mu(y) = \int_{\mathbf{\Lambda}>0} F_{\mu|\mathbf{\Lambda}}(y) f_{\mathbf{\Lambda}}(\mathbf{\Lambda})\,\mathrm{d}\mathbf{\Lambda}$ by deconditioning over $f_{\mathbf{\Lambda}}(\mathbf{\Lambda})$, i.e., the distribution of the unordered eigenvalues $\mathbf{\Lambda}$. We start by observing that when $n_\mathrm{r} \geq n_\mathrm{t}$, the eigenvalues of the kernel matrix $\mathbf{A}$ are specified by (7). In general, $\mathbf{A}$ has an eigenvalue $a = 0$ with multiplicity $n_\mathrm{r} - n_\mathrm{t} + 1$ and $n_\mathrm{t} - 1$ non-zero eigenvalues denoted by $\boldsymbol{\alpha} = [\alpha_1, \ldots, \alpha_{n_\mathrm{t}-1}]$. Therefore, $\mathbf{A}$ can be decomposed as $\mathbf{A} = \bar{\mathbf{U}}^\mathsf{H} \mathrm{diag}(\mathbf{a}) \bar{\mathbf{U}}$, where $\bar{\mathbf{U}}$ is a unitary matrix. By using such decomposition, we can write:

$$\mu = \frac{\mathbf{h}^\mathsf{H}\mathbf{A}\mathbf{h}}{\|\mathbf{h}\|^2} = \frac{\mathbf{h}^\mathsf{H}\bar{\mathbf{U}}^\mathsf{H}\mathrm{diag}(\mathbf{a})\bar{\mathbf{U}}\mathbf{h}}{\|\mathbf{h}^\mathsf{H}\bar{\mathbf{U}}^\mathsf{H}\|^2} = \frac{\tilde{\mathbf{h}}^\mathsf{H}\mathrm{diag}(\mathbf{a})\tilde{\mathbf{h}}}{\|\tilde{\mathbf{h}}\|^2}$$

where $\tilde{\mathbf{h}} = \bar{\mathbf{U}}\mathbf{h}$ has Gaussian i.i.d. entries since $\mathbf{h}$ is a vector of length n_r, with Gaussian i.i.d. entries. Furthermore, we have: $\frac{\tilde{\mathbf{h}}^\mathsf{H}\mathrm{diag}(\mathbf{a})\tilde{\mathbf{h}}}{\|\tilde{\mathbf{h}}\|^2} = \frac{\tilde{\mathbf{h}}_1^\mathsf{H}\mathrm{diag}(\boldsymbol{\alpha})\tilde{\mathbf{h}}_1}{\|\tilde{\mathbf{h}}_1\|^2+\|\tilde{\mathbf{h}}_2\|^2}$ where $\tilde{\mathbf{h}} = [\tilde{\mathbf{h}}_1^\mathsf{H}, \tilde{\mathbf{h}}_2^\mathsf{H}]^\mathsf{H}$, $\tilde{\mathbf{h}}_1$ has size $n_\mathrm{t} - 1$, and $\tilde{\mathbf{h}}_2$ has size $n_\mathrm{r} - n_\mathrm{t} + 1$. Let $z = \|\tilde{\mathbf{h}}_2\|^2$, then the cdf $F_{\mu|\mathbf{A}}(y) = \mathbb{P}(\mu \leq y|\mathbf{A})$ is given by $F_{\mu|\mathbf{A}}(y) = \int_0^\infty F_{\mu|\mathbf{A},z}(y) f_z(z)\,\mathrm{d}z$ by deconditioning over z. The distribution $F_{\mu|\mathbf{A},z}(y)$ is provided in [1, eq. (48)] as:

$$F_{\mu|\mathbf{A},z}(y) = u(yz) - \sum_{\ell=1}^{n_\mathrm{t}-1} \frac{(\alpha_\ell - y)^{n_\mathrm{t}-1} \mathrm{e}^{-\frac{yz}{\alpha_\ell - y}} u\left(\frac{yz}{\alpha_\ell - y}\right)}{|\alpha_\ell - y| \prod_{i=1, i\neq\ell}^{n_\mathrm{t}-1} (\alpha_\ell - \alpha_i)}$$

with $y > 0$, $z > 0$, and $u(\cdot)$ being the Heaviside step function. The density of y is specified in [27, Eq. (9)] and reads as: $f_z(z) = \frac{z^{n_\mathrm{r}-n_\mathrm{t}}}{(n_\mathrm{r}-n_\mathrm{t})!}\mathrm{e}^{-z}$. Thus, combining the above two expressions, the cdf $F_{\mu|\mathbf{A}}$ can be readily obtained as

$$\begin{aligned} F_{\mu|\mathbf{A}}(y) &= 1 - \sum_{\ell=1}^{n_\mathrm{t}-1} \frac{\int_0^\infty \mathrm{e}^{-\frac{yz}{\alpha_\ell - y}} u\left(\frac{yz}{\alpha_\ell - y}\right) \frac{z^{n_\mathrm{r}-n_\mathrm{t}}}{(n_\mathrm{r}-n_\mathrm{t})!}\mathrm{e}^{-z}\,\mathrm{d}z}{(\alpha_\ell - y)^{1-n_\mathrm{t}} |\alpha_\ell - y| \prod_{i=1, i\neq\ell}^{n_\mathrm{t}-1} (\alpha_\ell - \alpha_i)} \\ &= 1 - \sum_{\ell=1}^{n_\mathrm{t}-1} \frac{(\alpha_\ell - y)^{n_\mathrm{r}-1} u(\alpha_\ell - y)}{\alpha_\ell^{n_\mathrm{r}-n_\mathrm{t}+1} \prod_{i=1, i\neq\ell}^{n_\mathrm{t}-1} (\alpha_\ell - \alpha_i)}\,. \end{aligned} \quad (39)$$

Recall that $\alpha_i = (1+\lambda_i)^{-1}$ where λ_i are the eigenvalues of the channel matrix $\mathbf{G}^\mathsf{H}\mathbf{G}$. We then express $F_{\mu|\mathbf{A}}(y)$ through

the λ_i's. As for the factor $\prod_{i=1,i\neq\ell}^{n_\mathrm{t}-1}(\alpha_\ell-\alpha_i)$ in (39), we get:

$$\prod_{i=1,i\neq\ell}^{n_\mathrm{t}-1}(\alpha_\ell-\alpha_i)=\frac{(-1)^{n_\mathrm{t}-2}\prod_{i=1,i\neq\ell}^{n_\mathrm{t}-1}(\lambda_\ell-\lambda_i)}{(1+\lambda_\ell)^{n_\mathrm{t}-2}\prod_{i=1,i\neq\ell}^{n_\mathrm{t}-1}(1+\lambda_i)}\,. \quad (40)$$

Moreover, by using the definition of the Vandermonde determinant, it is easy to show that $\mathcal{V}(\mathbf{\Lambda}) = (-1)^{n_\mathrm{t}-1-\ell}\mathcal{V}(\mathbf{\Lambda}_\ell)\prod_{i=1,i\neq\ell}^{n_\mathrm{t}-1}(\lambda_\ell-\lambda_i)$ with $\mathbf{\Lambda}_\ell=\mathrm{diag}(\lambda_1,\ldots,\lambda_{\ell-1},\lambda_{\ell+1},\ldots,\lambda_{n_\mathrm{t}-1})$, $\ell=1,\ldots,n_\mathrm{t}-1$. Thus, (40) can be rewritten as:

$$\prod_{i=1,i\neq\ell}^{n_\mathrm{t}-1}(\alpha_\ell-\alpha_i)=\frac{(-1)^{\ell-1}}{(1+\lambda_\ell)^{n_\mathrm{t}-2}\prod_{i=1,i\neq\ell}^{n_\mathrm{t}-1}(1+\lambda_i)}\frac{\mathcal{V}(\mathbf{\Lambda})}{\mathcal{V}(\mathbf{\Lambda}_\ell)}\,.$$

By substituting in (39) all occurrences of α_i with $(1+\lambda_i)^{-1}$, the cdf $F_{\mu|\mathbf{\Lambda}}(y)$ now reads as

$$\begin{aligned}F_{\mu|\mathbf{\Lambda}}(y)&=1-\frac{1}{\mathcal{V}(\mathbf{\Lambda})}\sum_{\ell=1}^{n_\mathrm{t}-1}\frac{u\left(\frac{1}{1+\lambda_\ell}-y\right)(1+\lambda_\ell)^{n_\mathrm{t}-2}}{\left(\frac{1}{1+\lambda_\ell}-y\right)^{1-n_\mathrm{r}}\left(\frac{1}{1+\lambda_\ell}\right)^{\tau_1}(-1)^{\ell-1}}\\&\qquad\times\mathcal{V}(\mathbf{\Lambda}_\ell)\prod_{i=1,i\neq\ell}^{n_\mathrm{t}-1}(1+\lambda_i)\\&=1-\frac{1}{\mathcal{V}(\mathbf{\Lambda})}\sum_{\ell=1}^{n_\mathrm{t}-1}\frac{(-1)^{\ell+1}u\left(1-y(1+\lambda_\ell)\right)|\mathbf{W}_\ell|}{[1-y(1+\lambda_\ell)]^{1-n_\mathrm{r}}}\\&=1-\frac{|\mathbf{W}|}{\mathcal{V}(\mathbf{\Lambda})}\end{aligned} \quad (41)$$

where $|\mathbf{W}_\ell|=\mathcal{V}(\mathbf{\Lambda}_\ell)\prod_{i=1,i\neq\ell}^{n_\mathrm{t}-1}(1+\lambda_i)$ and $\mathbf{W}_\ell$ is an $(n_\mathrm{t}-2)\times(n_\mathrm{t}-2)$ matrix whose (i,j)-th element is given by $[\mathbf{W}_\ell]_{i,j}=(1+\lambda_i)\lambda_i^{j-1}$, for $i=1,\ldots,\ell-1,j=1,\ldots,n_\mathrm{t}-2$ and $[\mathbf{W}_\ell]_{i,j}=(1+\lambda_{i+1})\lambda_{i+1}^{j-1}$ for $i=\ell,\ldots,n_\mathrm{t}-2,j=1,\ldots,n_\mathrm{t}-2$. This result is obtained directly from the definition of the Vandermonde determinant and the Vandermonde matrix. Finally, the sum in the second line of (41) is the Laplace expansion on the first row of $\mathbf{W}$, defined as:

$$[\mathbf{W}]_{i,j}=\begin{cases}\dfrac{u\left(1-y(1+\lambda_i)\right)}{[1-y(1+\lambda_i)]^{1-n_\mathrm{r}}} & j=1,\ 1\leq i\leq n_\mathrm{t}-1\\ \lambda_i^{j-2}(1+\lambda_i) & 2\leq j\leq n_\mathrm{t}-1,\ 1\leq i\leq n_\mathrm{t}-1\,.\end{cases}$$

Equipped with the expression of $F_{\mu|\mathbf{\Lambda}}(y)$, we can now move to the second part of the proof, i.e., the computation of $F_\mu(y)$ by deconditioning over $\mathbf{\Lambda}$. It is clear that the expression of the integral that we have to compute to decondition with respect to $\mathbf{\Lambda}$, depends on the postulated $f_{\mathbf{\Lambda}}(\mathbf{\Lambda})$, which, in turn, is tailored to the specific scenario one has in mind. As done in Sec. IV, we assume the general model (12) for $f_{\mathbf{\Lambda}}(\mathbf{\Lambda})$.

We first evaluate $F_\mu(y)$ by using (12) and (41). We obtain:

$$\begin{aligned}F_\mu(y) &= \int_{\mathbf{\Lambda}>0}\left(1-\frac{|\mathbf{W}|}{\mathcal{V}(\mathbf{\Lambda})}\right)\frac{\mathcal{K}\mathcal{V}(\mathbf{\Lambda})|\mathbf{\Phi}|}{(n_\mathrm{t}-1)!}\prod_{i=1}^{n_\mathrm{t}-1}\psi(\lambda_i)\,\mathrm{d}\mathbf{\Lambda}\\&= 1-\frac{\mathcal{K}}{(n_\mathrm{t}-1)!}\int_{\mathbf{\Lambda}>0}|\mathbf{W}||\mathbf{\Phi}|\prod_{i=1}^{n_\mathrm{t}-1}\psi(\lambda_i)\,\mathrm{d}\mathbf{\Lambda}\\&= 1-\mathcal{K}|\bar{\mathbf{Q}}|\end{aligned}$$

where $\bar{\mathbf{Q}}$ is an $(n_\mathrm{t}-1)\times(n_\mathrm{t}-1)$ matrix whose entries can be computed by resorting to Lemma 3.2. More specifically,

$$[\bar{\mathbf{Q}}]_{i,j}=\begin{cases}\mathcal{I}_{j,n_\mathrm{r}-1}(y) & i=1,1\leq j\leq n_\mathrm{t}-1\\ \int_0^\infty\lambda^{i-2}\phi_j(\lambda)\psi(\lambda)(1+\lambda)\,\mathrm{d}\lambda & 2\leq i\leq n_\mathrm{t}-1\\ & 1\leq j\leq n_\mathrm{t}-1\end{cases}$$

where $\mathcal{I}_{j,n_\mathrm{r}-1}=\int_0^\infty\phi_j(\lambda)\psi(\lambda)\frac{u(1-y(1+\lambda))}{[1-y(1+\lambda)]^{1-n_\mathrm{r}}}\,\mathrm{d}\lambda$ can be conveniently written as in (38). Then the pdf of μ can readily be obtained as: $f_\mu(y)=\frac{\mathrm{d}}{\mathrm{d}y}F_\mu(y)=-\mathcal{K}\frac{\mathrm{d}}{\mathrm{d}y}|\bar{\mathbf{Q}}|$. Since $-\frac{\mathrm{d}}{\mathrm{d}y}$ is a linear operator and only the first column of $\bar{\mathbf{Q}}$ depends on y, we can apply the result in Lemma 3.1 and obtain (36) where

$$[\mathbf{Q}]_{i,j}=\begin{cases}-\frac{\mathrm{d}}{\mathrm{d}z}[\bar{\mathbf{Q}}]_{i,j} & i=1,1\leq j\leq n_\mathrm{t}-1\\ [\bar{\mathbf{Q}}]_{i,j} & 2\leq i\leq n_\mathrm{t}-1,1\leq j\leq n_\mathrm{t}-1\,.\end{cases}$$

Note that, for $i=1,1\leq j\leq n_\mathrm{t}-1$, the term $-\frac{\mathrm{d}}{\mathrm{d}y}[\bar{\mathbf{Q}}]_{i,j}=-\frac{\mathrm{d}}{\mathrm{d}y}\mathcal{I}_{j,n_\mathrm{r}-1}(y)=(n_\mathrm{r}-1)\mathcal{I}_{j,n_\mathrm{r}-2}(y)$. Thus the matrix $\mathbf{Q}$ can be rewritten as in (37). ■

A. Rayleigh-faded interferers

We start the analysis from the case of uncorrelated Rayleigh-faded interference. This translates into $\widehat{\mathbf{H}}$ following a standard multivariate complex Gaussian distribution, with uncorrelated elements. When $\widehat{\mathbf{\Delta}}=\sqrt{\hat{\delta}}\mathbf{I}$, the joint distribution of the $n_\mathrm{t}-1$ (unordered) non-zero random eigenvalues of $\mathbf{G}^\mathsf{H}\mathbf{G}$ can be written as (21). By comparing (21) to (12), we identify the following terms: $\phi_j(\lambda)=\lambda^{j-1}$, $\psi(\lambda)=\frac{\lambda^{n_\mathrm{r}-n_\mathrm{t}+1}}{\hat{\delta}^{n_\mathrm{r}}}\mathrm{e}^{-\lambda/\hat{\delta}}$, and $\mathcal{K}=\mathcal{K}_1=\frac{\pi_{n_\mathrm{t}-1}^2}{\Gamma_{n_\mathrm{t}-1}(n_\mathrm{t}-1)\Gamma_{n_\mathrm{t}-1}(n_\mathrm{r})}$. These terms, replaced in (36)–(38), provide $F_\mu(y)=1-\mathcal{K}_1|\bar{\mathbf{Q}}_1|$ with

$$[\bar{\mathbf{Q}}_1]_{i,j}=\begin{cases}\dfrac{v^{n_\mathrm{r}+\tau_j}(n_\mathrm{r}-1)!\tau_j!{}_1F_1\left(n_\mathrm{r};n_\mathrm{r}+\tau_j+1;\frac{v}{\hat{\delta}}\right)}{y^{1-n_\mathrm{r}}\hat{\delta}^{n_\mathrm{r}}\mathrm{e}^{v/\hat{\delta}}(n_\mathrm{r}+\tau_j)!} & i=1,\ 1\leq j\leq n_\mathrm{t}-1\\ \hat{\delta}^{i+j-1-n_\mathrm{t}}\left[(i+\tau_j-2)!+\hat{\delta}(i+\tau_j-1)!\right] & 2\leq i\leq n_\mathrm{t}-1,\ 1\leq j\leq n_\mathrm{t}-1\end{cases}$$

B. Spatially correlated interferers

Moving to a slightly less homogeneous scenario, we postulate that, while the useful signal stream undergoes uncorrelated Rayleigh fading, interference is coming from a bunch of spatially correlated and Rayleigh faded transmitters. This occurs, e.g., when interfering transmitters are located in close proximity to each other, but well spatially separated from the useful signal source. In such a case, the distribution of the unordered, non-zero eigenvalues of $\mathbf{G}\mathbf{G}^\mathsf{H}$ is given by (26), which, compared to (12), allows us to identify the following terms $\phi_j(\lambda_i)=\mathrm{e}^{-\lambda_i/\sigma_j}$, $\psi(\lambda)=\lambda^{n_\mathrm{r}-n_\mathrm{t}+1}$, and $\mathcal{K}=\mathcal{K}_2=\frac{\pi_{n_\mathrm{t}-1}}{\Gamma_{n_\mathrm{t}-1}(n_\mathrm{r})\mathcal{V}(\mathbf{\Sigma})|\mathbf{\Sigma}|^{n_\mathrm{r}-n_\mathrm{t}+2}}$. We recall that $\mathbf{\Sigma}$ is the common covariance of each row of $\mathbf{G}$ whose eigenvalues are denoted by $\{\sigma_1,\ldots,\sigma_{n_\mathrm{t}-1}\}$. By substituting these results in (36), we obtain $F_\mu(y)=1-\mathcal{K}_2|\bar{\mathbf{Q}}_2|$ where

$$[\bar{\mathbf{Q}}_2]_{i,j}=\begin{cases}\dfrac{(n_\mathrm{r}-1)!\tau_1!{}_1F_1\left(n_\mathrm{r};2n_\mathrm{r}-n_\mathrm{t}+2;\frac{v}{\sigma_j}\right)}{v^{n_\mathrm{t}-2n_\mathrm{r}-1}y^{1-n_\mathrm{r}}\mathrm{e}^{v/\sigma_j}(2n_\mathrm{r}-n_\mathrm{t}+1)!} & i=1,\ 1\leq j\leq n_\mathrm{t}-1\\ (i+\tau_{-1})!\sigma_j^{i+n_\mathrm{r}-n_\mathrm{t}}[1+\sigma_j(i+n_\mathrm{r}-n_\mathrm{t})] & 2\leq i\leq n_\mathrm{t}-1,\ 1\leq j\leq n_\mathrm{t}-1\,.\end{cases}$$

C. Other fading distributions

For brevity, we do not report here the cases of Rice and multiscattering fading distributions. However, they can be easily obtained by using the corresponding eigenvalue distributions and by plugging them into (14).

VIII. Numerical results on the ME gap

We now validate our analysis of the ME gap through numerical simulation.

Fig. 5(left) depicts the pdf and the cdf of the ME gap when both the useful and interfering signals are affected by Rayleigh fading. We set $n_{\rm r}=6$, $n_{\rm t}=4$, while $\hat{\delta}$ varies. The perfect match between analytical and simulation results confirms the validity of our derivations. Also, as expected, for decreasing values of the SNR δ, the gap in performance between the MMSE and the ZF receivers grows. Similar observations hold for Fig. 5(right), which presents the cdf of the ME gap for $n_{\rm r}=8$, $n_{\rm t}=2,4,6,8$, and $\sigma_j=\frac{2j}{n_t(n_t-1)}$. Note that larger values of the ME gap become significantly more likely as the number of interfering streams (i.e., n_t) increases.

Fig. 6 shows the cdf of the ME gap when both $n_{\rm t}$ and $n_{\rm r}$ increase, the ratio $n_{\rm t}/n_{\rm r}=2/3$ is fixed, and the interfering signals are affected by Rayleigh fading. The analytical and simulation results coincide and show the improvement in performance as the number of antennas increases. Interestingly, as the number of antennas increases, the cdf of the ME gap tends to a Heaviside step function around the asymptotic value of the gap. We then address the massive MIMO scenario more extensively in the next section.

IX. Gaps statistics in doubly massive settings

Here, we discuss the extension of our results to the *doubly massive* MIMO setting, i.e., to the case where both n_t and n_r grow large with a fixed ratio, i.e., $\lim_{n_t,n_r\to\infty}\frac{n_t-1}{n_r}=\beta\leq 1$. We start by focusing on the SINR gap and define $\nu_\infty=\lim_{n_r\to\infty}\frac{\nu}{n_{\rm r}}$ where ν is as in (5). Also, for simplicity, let us initially consider a finite number of interfering nodes, N, each with a finite and common budget of transmission power, $\widetilde{\delta}$, and equipped with $(n_{\rm t}-1)/N$ antennas. Hence, $\hat{\delta}=\widetilde{\delta}N/(n_{\rm t}-1)$ and

$$\frac{\nu}{n_{\rm r}}=\beta\delta\mathbf{w}^{\mathsf{H}}\left(\mathbf{I}+\frac{\widetilde{\delta}N}{\beta}\frac{\mathbf{L}}{n_{\rm r}}\right)^{-1}\mathbf{w}$$

where $\mathbf{w}=\mathbf{U}^{\mathsf{H}}\mathbf{h}/(n_{\rm t}-1)$ is a complex Gaussian random vector of length $n_{\rm t}-1$, with independent entries with zero-mean, and variance equal to $\frac{1}{n_{\rm t}-1}$. Then, by virtue of [31, Lemma(2.29.b)], as $n_{\rm r}\to\infty$ and if the spectra of $\widetilde{\mathbf{L}}=\mathbf{L}/n_{\rm r}$ converge, we have

$$\nu_\infty=\beta\delta\eta_{\widetilde{\mathbf{L}}}\left(\frac{\widetilde{\delta}N}{\beta}\right). \tag{42}$$

The availability of a closed-form expression for $\eta_{\widetilde{\mathbf{L}}}\left(\frac{\widetilde{\delta}N}{\beta}\right)$ determines the possibility of explicitly characterizing the SINR gap in the doubly-massive setting. In our case, either assuming independent Rayleigh or Rice fading affecting the interfering signals, by [31, Example (2.10)], we obtain

$$\eta_{\widetilde{\mathbf{L}}}(x)=1-\frac{\left(\sqrt{x(1+\sqrt{\beta})^2+1}-\sqrt{x(1-\sqrt{\beta})^2+1}\right)^2}{4\beta x}. \tag{43}$$

In the Rice case, however, besides assuming $\mathbf{\Omega}$ to have fixed rank $1\leq r\leq n_t-1$, one must enforce that $\lim_{n_t\to\infty}\frac{r}{n_t-1}=0$; this is a direct consequence of [31, Lemma(2.22), Th.(2.49)]. Note also that the same statistical behavior as in (43) can be observed if the entries of the channel matrix are independent but non-identically distributed, with variances satisfying some mild constraints (see, again, [31, Th.(2.49)]). This case allows us to relax our initial assumption on equally distributed interfering powers.

In the case of correlated Rayleigh fading, (42) takes on a more involved expression, which can be obtained by solving a fixed-point equation provided by [31, Eq.(2.124)]. Finally, in the presence of multiple scattering, ν_∞ can only be explicitly evaluated when the interferers' matrix is a product of up to 3 independent matrix factors. However, to get a properly normalized asymptotic model, and according to the notation adopted in Sec. IV-C, matrices $\mathbf{K}_i$'s are required to have i.i.d. complex zero-mean Gaussian entries, with variance proportional to $1/n_i$. Fig. 7 shows the cdf of the normalized SINR gap, $\nu/n_{\rm r}$, as the number of antennas increases, and its asymptotic value ν_∞ for $\beta=1/2$. It is evident that, as $n_{\rm t}$ and $n_{\rm r}$ grow large, the cdf of the normalized gap tends to the Heaviside step function centered at ν_∞, thus confirming the validity of our derivation.

As far as the ME is concerned, similarly to the SINR gap, we can define $\mu_\infty=\lim_{n_{\rm r}\to\infty}\mu$ where a further normalization is not required due to the presence in (6) of the term at the denominator. The asymptotic characterization of μ_∞ is more complicated than that of ν_∞, and can be performed just in a more restrictive framework. Indeed, it can be carried out by exploiting [31, Theorems (2.50-56)], which encompass the broad class of channels matrices with independent and non-identically distributed entries. Uncorrelated Rayleigh and Rician fading cases fall within this framework, while correlated entries or multiple scattering have to be separately addressed through an analysis that goes beyond this work.

X. Conclusions

We considered scenarios in which transmitter and receiver, as well as interfering nodes, may be equipped with multiple antennas, and either the MMSE or the ZF filter is used at the receiver. In these scenarios, we evaluated the relative performance of the two receivers by looking at two important metrics, namely, the SINR gap and the ME gap. For the first time in this work, we characterized such statistics in closed form under finite-size setting. We derived these results by leveraging the expressions of the SINR and ME gap in terms of quadratic forms in random matrices whose kernel depends only on the interfering signals. Interestingly, the closed-form distribution of the aforementioned performance metrics turned out to be elegant, compact expressions, given by the product of a constant by the determinant of the communication system

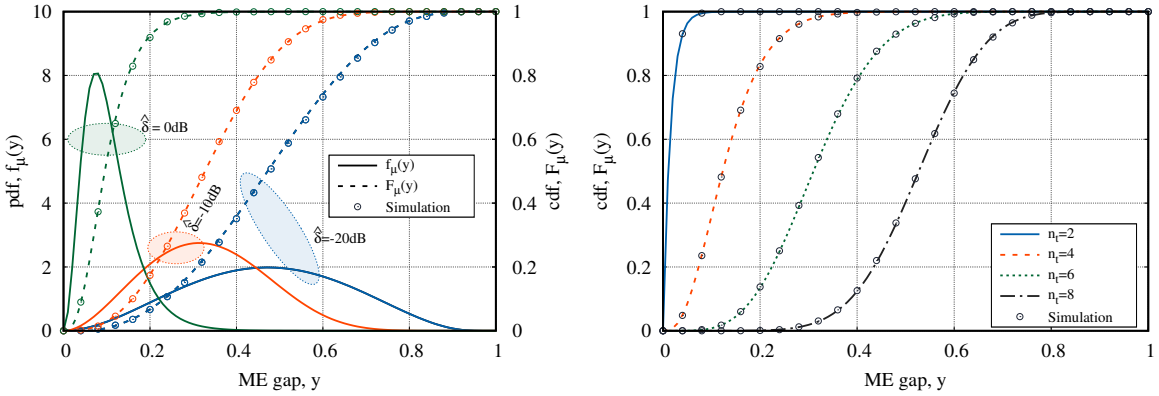

Fig. 5. Left: pdf and cdf of the ME gap for Rayleigh channel with $n_\mathrm{r} = 6$, $n_\mathrm{t} = 4$, and varying values of $\hat{\delta}$. Right: cdf of the ME gap for correlated Rayleigh channel, with $n_\mathrm{r} = 8$ and $n_\mathrm{t} = 2, 4, 6, 8$.

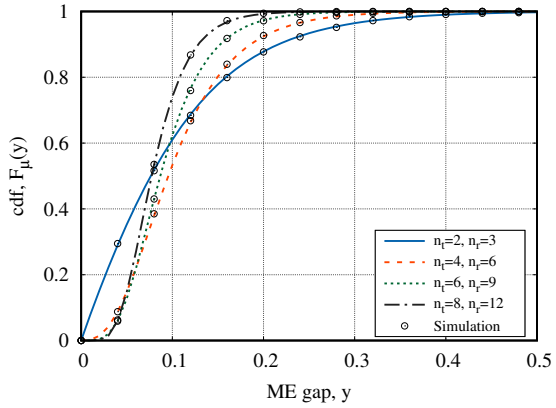

Fig. 6. Cdf of the ME gap as the number of transmit and receive antennas varies, for Rayleigh interfering channel.

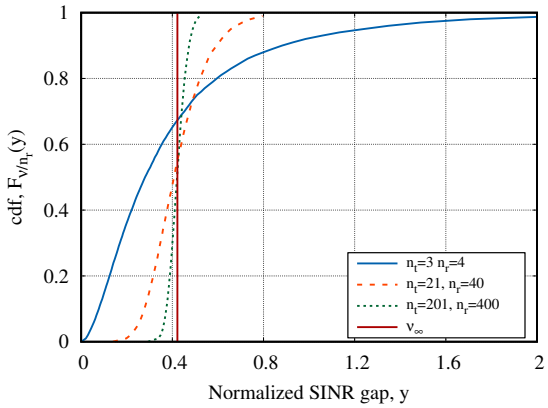

Fig. 7. Cdf of the normalized SINR gap as n_t and n_r vary, for Rayleigh interfering channel.

matrix. The results have been first obtained under general fading distribution affecting the interfering signals, and then they have been specialized to the cases of Rayleigh, Rice, and multiscattering channel. In order to tackle next-generation wireless systems, we also provided some results and discussion on the SINR and ME gaps in the doubly massive MIMO scenario. Finally, we validated our analytical results through Monte Carlo simulations, and we exploited them to derive the error and outage probability of the system.

Appendix A
Derivation of the Expression of the SINR Gap in (5)

By definition of $\mathbf{H}$ and $\mathbf{\Delta}$, we have $\mathbf{H\Delta} = [\sqrt{\delta}\mathbf{h}, \mathbf{G}]$, where $\mathbf{G} = \widehat{\mathbf{H}}\widehat{\mathbf{\Delta}}$. Then

$$\mathbf{I} + \mathbf{\Delta}\mathbf{H}^\mathsf{H}\mathbf{H}\mathbf{\Delta} = \begin{bmatrix} 1+\delta|\mathbf{h}|^2 & \sqrt{\delta}\mathbf{h}^\mathsf{H}\mathbf{G} \\ \sqrt{\delta}\mathbf{G}^\mathsf{H}\mathbf{h} & \mathbf{I}+\mathbf{G}^\mathsf{H}\mathbf{G} \end{bmatrix}.$$

Let $\mathbf{B} = \mathbf{I} + \mathbf{\Delta}\mathbf{H}^\mathsf{H}\mathbf{H}\mathbf{\Delta}$. By exploiting the results on block matrix inversion, we get

$$[\mathbf{B}^{-1}]_{1,1} = \left(1+\delta|\mathbf{h}|^2 - \delta\mathbf{h}^\mathsf{H}\mathbf{G}(\mathbf{I}+\mathbf{G}^\mathsf{H}\mathbf{G})^{-1}\mathbf{G}^\mathsf{H}\mathbf{h}\right)^{-1}.$$

Thus, the SINR γ^{MMSE} in (1) can be rewritten as $\gamma^{\mathrm{MMSE}} = \delta|\mathbf{h}|^2 - \delta\mathbf{h}^\mathsf{H}\mathbf{G}(\mathbf{I}+\mathbf{G}^\mathsf{H}\mathbf{G})^{-1}\mathbf{G}^\mathsf{H}\mathbf{h}$, and $(\mathbf{\Delta}\mathbf{H}^\mathsf{H}\mathbf{H}\mathbf{\Delta})^{-1}]_{1,1} = \left(\delta|\mathbf{h}|^2 - \delta\mathbf{h}^\mathsf{H}\mathbf{G}(\mathbf{G}^\mathsf{H}\mathbf{G})^{-1}\mathbf{G}^\mathsf{H}\mathbf{h}\right)^{-1}$. Then, $\nu = \gamma^{\mathrm{MMSE}} - \gamma^{\mathrm{ZF}}$, which is equal to $\delta\mathbf{h}^\mathsf{H}\mathbf{G}\left[(\mathbf{G}^\mathsf{H}\mathbf{G})^{-1} - (\mathbf{I}+\mathbf{G}^\mathsf{H}\mathbf{G})^{-1}\right]\mathbf{G}^\mathsf{H}\mathbf{h}$. Letting $\mathbf{G}=\mathbf{U}\mathbf{\Lambda}^{1/2}\mathbf{V}^\mathsf{H}$ and after some algebra, we get (5).

References

[1] T. Y. Al-Naffouri, M. Moinuddin, N. Ajeeb, B. Hassibi, A. Moustakas, "On the Distribution of Indefinite Quadratic Forms in Gaussian Random Variables," *IEEE Transactions on Communications*, Vol. 64, No. 1, pp. 153–165, 2016.

[2] Y. Jian, M. K. Varanasi, J. Li, "Performance Analysis of ZF and MMSE Equalizers for MIMO Systems: An In-Depth Study of the High SNR Regime," *IEEE Transactions on Information Theory*, Vol. 57, No. 4, pp. 6788–6805, 2011.

[3] P. Li, D. Paul, R. Narasimhan J. Cioffi "On the Distribution of SINR for the MMSE MIMO Receiver and Performance Analysis," *IEEE Transactions on Information Theory*, Vol. 52, No. 1, pp. 271–286, 2006.

[4] A. Tulino, L. Li, S. Verdù, "Spectral Efficiency of Multicarrier CDMA," *IEEE Trans. on Inf. Th.*, Vol. 51, No. 2, pp. 479–505, 2005.

[5] H. Tataria, *et al.*, "Impact of Line-of-sight and Unequal Spatial Correlation on Uplink MU-MIMO Systems," *IEEE Wireless Comm. Lett.*, Vol. 6, No. 5, pp. 634–637, Oct. 2017.

[6] H. Tataria, *et al.*, "Revisiting MMSE Combining for Massive MIMO Over Heterogeneous Propagation Channels," *IEEE ICC*, Kansas City, 2018.

[7] P. C. B. Phillips, "The True Characteristic Function of the F Distribution," *Biometrika*, Vol. 69, No. 1, pp. 261–264, 1982.

[8] D. A. Gore, R. W. Heath, A. J. Paulraj, "Transmit Selection in Spatial Multiplexing Systems," *IEEE Communications Letters*, Vol. 6, No. 11, pp. 491–493, 2002.

[9] C. Siriteanu, S. D. Blostein, A. Takemura, H. Shin, S. Yousefi, S. Kuriki, "Exact MIMO Zero-forcing Detection Analysis for Transmit-correlated Rician Fading," *IEEE Transactions on Wireless Communications*, Vol. 13, No. 3, pp. 1514–1527, 2014.

[10] C. Siriteanu, A. Takemura, S. Kuriki, D. St. P. Richards, H. Shin, "Schur Complement Based Analysis of MIMO Zero-forcing for Rician Fading," *IEEE Transactions on Wireless Communications*, Vol. 14, No. 4, pp. 1757–1771, 2015.

[11] R. Müller, "Multiuser Receivers for Randomly Spread Signals: Fundamental Limits with and without Decision-Feedback," *IEEE Transactions on Information Theory,* Vol. 47, No. 1, pp. 268–283, 2001.

[12] N. Kim, Y. Lee, H. Park, "Performance Analysis of MIMO System with Linear MMSE Receiver," *IEEE Transactions on Wireless Communications,* Vol. 7, No. 11, pp. 4474–4478, Nov. 2008.

[13] H. Gao, P. J. Smith, M. V. Clark, "Theoretical Reliability of MMSE Linear Diversity Combining in Rayleigh-fading Additive Interference Channels," *IEEE Transactions on Communications* Vol. 46, No. 5, pp. 666–672, 2003.

[14] M. R. McKay, A. Zanella, I. B. Collings, M. Chiani, "Error Probability and SINR Analysis of Optimum Combining in Rician Fading," *IEEE Transactions on Communications*, Vol. 57, No. 3, pp. 676–687, 2009.

[15] A. L. Moustakas, "Tails of Composite Random Matrix Diagonals: The Case of the Wishart Inverse," *Acta Physica Polonica B*, Vol. 42, No. 5, Apr. 2011.

[16] G. Akemann, J. Ipsen, M. Kieburg, "Products of Rectangular Random Matrices: Singular Values and Progressive Scattering," *APS Physics Review E*, Vol. 88, No. 3, 2013.

[17] H. Shin, M. Z. Win, "MIMO Diversity in the Presence of Double Scattering," *IEEE Transactions on Information Theory* Vol. 54, No. 7, pp. 2976–2996, 2008.

[18] C. Zhong, T. Ratnarajah, Z. Zhang, K.-K. Wong, M. Sellathurai, "Performance of Rayleigh Product MIMO Channels with Linear Receivers," *IEEE Transactions on Wireless Communications*, Vol. 13, No. 4, pp. 2270–2281, 2014.

[19] G. Alfano, C.-F. Chiasserini, A. Nordio, "Rayleigh Quotient Based Analysis of MIMO Linear Receivers," *WSA*, Berlin, Germany, pp. 1-6, 2017.

[20] I. S. Gradshteyn, I. M. Ryzhik, *Table of Integrals, Series, and Products*, Academic Press, New York, 1980.

[21] A. T. James, "Distribution of Matrix Variates and Latent Roots Derived from Normal Samples," *Ann. Math. Stat.,* Vol. 35, No. 2, pp. 474–501, 1964.

[22] S. Verdú, *Multiuser Detection*, Cambridge University Press, 2011.

[23] P. J. Smith, L. M. Garth, S. Loyka,"Exact Capacity Distributions for MIMO Systems with Small Numbers of Antennas," *IEEE Communications Letters*, Vol. 7, No. 10, pp. 481–483, 2003.

[24] R. A. Horn and C. R. Johnson, *Matrix Analysis*, Cambridge, MA: Cambridge Univ. Press, 1985.

[25] M. Chiani, M. Z. Win, A. Zanella, "On the Capacity of Spatially Correlated MIMO Rayleigh-fading Channels," *IEEE Transactions on Information Theory,* Vol. 49, No. 10, pp. 2363–2371, 2003.

[26] H. Gao and P. J. Smith, "A Determinant Representation for the Distribution of Quadratic Forms in Complex Normal Vectors," *Journal Mult. Anal.* Vol. 73, No. 2, pp. 96—103, 2003.

[27] G. Alfano, C.-F. Chiasserini, A. Nordio, S. Zhou, "Closed-Form Output Statistics of MIMO Block-Fading Channels," *IEEE Transactions on Information Theory,* Vol. 60, No. 12, pp. 7782–7797, 2014.

[28] S. Jin, M. R. McKay, X. Gao, I. B. Collings, "MIMO Multichannel Beamforming: SER and Outage Using New Eigenvalue Distributions of Complex Noncentral Wishart Matrices," *IEEE Trans. on Comm.*, Vol. 56, No. 3, pp. 424–434, 2008.

[29] M. Matthaiou, P. de Kerret, G. Karagiannidis, J. Nossek, "Mutual Information Statistics and Beamforming Performance Analysis of Optimized LoS MIMO Systems," *IEEE Trans. on Wireless Comm.*, Vol. 58 No. 11, pp. 3316–3329, 2010.

[30] G. Alfano, C. Chiasserini, A. Nordio, and S. Zhou, "Information-Theoretic Characterization of MIMO Systems With Multiple Rayleigh Scattering," *IEEE Transactions on Information Theory*, Vol. 64, No. 7, pp. 5312–5325, 2018.

[31] A. Tulino and S. Verdú, "Random Matrices and Wireless Communications," *Foundations and Trends in Communications and Information Theory,* Vol. 1, No. 1, July 2004.